https://doi.org/10.5194/acp-2022-199
Preprint. Discussion started: 11 April 2022

Atmospheric Chemistry and Physics Discussions
Open Access

Insight into seasonal aerosol concentrations, meteorological influence, and transport over the Pan-Third Pole region using multi-sensors satellite and model simulation

Mukesh Rai[1, 2], Shichang Kang[1, 2*], Junhua Yang[1], Maheswar Rupakheti[4], Dipesh Rupakheti[3], Lekhendra Tripathee[1], Yuling Hu[1], Xintong Chen[1, 2]

[1]*State Key Laboratory of Cryospheric Science, Northwest Institute of Eco-Environment and Resources, Chinese Academy of Sciences, Lanzhou 730000, China*

[2]*University of Chinese Academy of Sciences, Beijing 100049, China*

[3]*Jiangsu Key Laboratory of Atmospheric Environment Monitoring and Pollution Control, Collaborative Innovation Center of Atmospheric Environment and Equipment Technology, School of Environmental Science and Engineering, Nanjing University of Information Science & Technology, Nanjing 210044, China*

[4]*Institute for Advanced Sustainability Studies, Potsdam, Germany*

*Corresponding author:

shichang.kang@lzb.ac.cn (S. Kang)

Key points:

- Prolonged winter dominance of aerosols favored by both meteorology and emissions.
- A columnar abundance of aerosols was found to be maximum within 1-2 km over South Asia and Eastern China that can be injected into the free troposphere.
- Integrated BC and OC aerosol transport were dominant over Southeast Asia with OC anomaly during spring (~5 times > mean), however, the maximum Dust aerosol transport was found over arid land and desert.

https://doi.org/10.5194/acp-2022-199
Preprint. Discussion started: 11 April 2022

Abstract

The Pan-Third Pole (PTP) owns complex geography and demographic features where aerosol roles and their impact cannot be neglected as it jeopardizes both the environment and human health. Therefore, we analyzed spatio-temporal aerosol concentration, the influence of meteorological conditions, and underlying aerosol transport mechanisms over the PTP by leveraging observation, satellite dataset, and model outputs. The observation and model simulation result showed that aerosol concentrations exceeded the world health organization (WHO) and China guideline values in most of the locations. This study revealed distinctive seasonality with the highest and lowest aerosol concentrations during the winter and summer seasons, respectively, which could be favored by meteorological conditions and emissions from biomass burning. In response to higher aerosol concentrations, the maximum aerosol optical depth (AOD) values were observed over the major hotspot regions however, interestingly summer high (AOD > 0.8) was observed over the Indo Gangetic Plain (IGP) in South Asia. The columnar aerosol profile indicated that the higher aerosol concentrations were limited within 1-2 km elevation over the densely populated regions over South Asia and Eastern China. However, the significant aerosols concentrations found to be extended as high as 10 km could potentially be driven by the deep convection process and summer monsoon activities. Regionally, the integrated aerosol transport (IAT) for black carbon (BC) and organic carbon (OC) was found to be maximum over SA. Noticeable OC IAT anomaly (~5 times > annual mean) found during spring that was linked with the biomass burning events. Yet, the dust transportation was found to be originated from the arid land and deserts that prolonged especially during summer followed by spring seasons. This study highlights the driver mechanism in aerosol seasonality, transport mechanism, and further motivates the additional assessment into potential dynamic relation between aerosol species, aerosol atmospheric river, and its societal impact.

Keywords: *Aerosols, AOD, IAT, Pan-Third Pole, transport dynamics, WRF-Chem*

https://doi.org/10.5194/acp-2022-199
Preprint. Discussion started: 11 April 2022

1. Introduction

On a regional to the global scale, the atmospheric aerosol has been a major research topic over the recent decades as aerosol impacts ecosystems, climate, and human health. Either way, direct or indirect interaction aerosols perturb the amount of solar radiation reaching the Earth's surface (Twomey, 1977; Haywood and Boucher, 2000; Charlson et al., 1992). The nexus between poor air quality and adverse health outcomes have been documented by epidemiological studies (Shiraiwa et al., 2017; Ravishankara et al., 2020; Lelieveld et al., 2015; Jerrett, 2015; Hong et al., 2019). Globally, ambient air pollution is a major health risk as several adverse health outcomes are linked with poor air quality (Chen et al., 2018; Manisalidis et al., 2020). Due to exposure to ambient air pollution, 4.2 million premature deaths have been reported worldwide in a year in 2016 (Who, 2021). Earlier studies articulate the significant aerosol loadings over Asia and its impact (Ramanathan et al., 2007; Carmichael et al., 2009). The regions with population density in South Asia (SA) and East China (EC) face episodic acute air pollution events that are primarily brought forth by a dramatic increase in emissions from rapid urbanization, industrial expansion, power generation, and transportation sectors (Kumar et al., 2020; Yang et al., 2020). Recent events like a super sandstorm in China (Yin et al., 2021; Liu et al., 2021), haze pollution in Delhi (Jena et al., 2021; Dhaka et al., 2020), and extreme air pollution in Kathmandu (Islam et al., 2020; Putero et al., 2015) again raised the prominent concern among all environmental issues over the region.

The Pan-Third Pole (PTP) comprises relatively pristine Himalayas and Tibetan Plateau (HTP) but is it surrounded by arid regions to the west and highly polluted regions like Indo-Gangetic Plain (IGP) to the south. The significant aerosol concentrations found over the background region (i.e., HTP) are mainly driven by long-range transport (Yang et al., 2018; Zhang et al., 2015a; Han et al., 2020; Gabrielli et al., 2020). Aerosols like black carbon (BC) and dust could enhance glacier melting thereby posing threat to the hydrological cycle and water availability (Kang et al., 2010; Menon et al., 2002; Ming et al., 2008; Sarangi et al., 2020; Kang et al., 2019). Thus, the fate of cryospheric bodies also depends on the transport of emissions from upwind source regions. Other than this, the complex interplay of aerosols is associated with hydrological processes. It is reported that an increase in aerosol loading and their effects on radiation and cloud microphysics can lead to a weaker Asian hydrological cycle and reduce monsoon precipitation (Ramanathan et al., 2001; Takahashi et al., 2018). A comprehensive review gives more insights into interactions between Asian aerosols and monsoon (Li et al., 2016b).

In light of the aforementioned evidence of aerosol impacts, attempts have been made from the quantification of aerosol physical, chemical, optical, and radiative properties to understand the relation between cause and effect of severe air quality over Asia, of which, the majority of studies are mainly focused on the highly polluted regions in South Asia (Ojha et al., 2020; Moorthy et al., 2005; Kumar et al., 2015; Ghude et al., 2016; Ramachandran et al., 2020b) and East China (Huang et al., 2020; Uno et al., 2020; Dang and Liao, 2019; Ding et al., 2016). However, in a relatively cleaner region (i.e., HTP) such potential impacts have gained attention only recently. To quantify the source-receptor transport mechanism over the HTP, the emission perturbation (Yang et al., 2018; Han et al., 2020), backward-trajectory (Lüthi et al., 2015; Lu et al., 2012), tracer-tagging (Kumar et al., 2015; Zhang et al., 2015b), and adjoint (Kopacz et al., 2011) method has been deployed.

Also, more studies have been carried out taking into account the aerosol impact on meteorology and vice versa (Zheng et al., 2015; Vinoj and Pandey, 2022; Yuan et al., 2020; Zhao et al., 2017; Huang et al., 2018; Ojha et al., 2020; Lv et al., 2020). As stated by Kumar et al. (2018), Representative Concentration Pathways (RCP) scenarios project a global improvement in air quality, while it will continue to deteriorate over SA over at least the next two decades. It was found that $PM_{2.5}$ (particulate matter with aerodynamic diameter $\leq$ 2.5 μm) will increase across South Asia due to the combined effects of the increase in emissions of air pollutants and meteorological conditions under RCP8.5. Kulkarni et al. (2015) also stated that worsening air quality in coming days over SA continues to breach the WHO guideline values. The same study projected that $PM_{2.5}$ decreases over EC and increases significantly in South Asia and Central Asia under the reference scenario (2030). The national air quality observation database and modeling studies indicate that there is a significant decrease of ambient $PM_{2.5}$ concentrations over China (Ding et al., 2019; Uno et al., 2020; Kanaya et al., 2020; Fan et al., 2020; Kong et al., 2021; Zhang et al., 2019a) which also supported by RCP scenario projection study as well (Li et al., 2016a). Whereas, multiple inter-comparison of Aerosol Optical Depth (AOD) data from 2003 to 2017 also indicated an increasing trend over South Asia while decreasing in East China (Gui et al., 2021; Li, 2020). In addition, the PTP region includes the number of deserts and arid regions that are the primary source of natural dust emissions and a significant contributor to ambient particulate matter (Chinnam et al., 2006; Ginoux et al., 2001; Chen et al., 2017). Over the PTP region, numerous systematic efforts have been made for the analysis of dust sources, transport, and impact of dust on radiation budget and glaciers in the region (Kumar et al., 2014; Zhang et al., 2020b; Zhao et al., 2010; Li and Sokolik, 2018; Chen et al., 2017; Nabavi et al., 2017; Parajuli et al., 2019)

The PTP is highly vulnerable from a climate and human dimension perspective. However, given its fragile ecosystems of global importance the region has not received the attention it deserves in terms of deteriorating air pollution in and around the PTP. Owing to complex geography from low land, arid, semi-arid to high mountain regions where the aerosol burden from surface to the upper troposphere and lower stratosphere over the PTP region from emissions associated with human and natural activities that is processed under the dynamic and vigorous transport mechanisms leads to intricate aerosol-geography-radiation-cloud-climate interactions over the region that are yet to be understood properly. The majority of past studies focused on East China and South Asia regions. However, synoptic-scale studies covering the PTP are scarce which reflects the necessity of further investigation of aerosol distribution, aerosol climatology, long-range transport, and topographic effect on a seasonal basis across the PTP and quantifying contributions of various mechanisms and processes. Therefore, here we used a combination of observations, state-of-art Weather Research and Forecasting coupled with the Chemistry (WRF-Chem) model, the Hybrid Single-Particle Lagrangian Integrated Trajectory (HYSPLIT) model, and the Image-Processing-based Atmospheric River Tracking (IPART) module. To our knowledge, this paper attempts to offer for the first time the quantification of integrated aerosol transport (IAT) using the IPART module for the PTP region. The main objectives of this study are: (1) to evaluate the performance of the model (WRF-Chem), and (2) to understand the spatio-temporal distribution, vertical profile, meteorological influence, and transport mechanism of aerosols ($PM_{2.5}$, PM_{10}, organic compound (OC), BC, and dust). We anticipate that our study helps to bridge the gap in the understanding of a complex interplay between aerosols-climate and associated impacts over the region of global significance. The paper is organized as follows. The details on model setup and observation data used in the study are described in Sec. 2. The spatio-temporal distributions and transport processes are analyzed in Sec. 3. The major findings from the study are summarized in Sec. 4.

2. Methods

2.1. WRF-Chem model

In this study, WRF-Chem (version 3.6), a mesoscale three-dimensional Eulerian chemical transport model which enables the feedback between meteorology and chemical processes was

https://doi.org/10.5194/acp-2022-199
Preprint. Discussion started: 11 April 2022

used (Skamarock et al., 2005; Grell et al., 1994). We conducted a numerical simulation in a domain with 150 × 208 horizontal grids with a horizontal resolution of 30 km for the simulation of $PM_{2.5}$, PM_{10}, OC, dust, and meteorological parameters. The model has 40 vertical sigma levels from the surface to the top of the level (50 hPa). The initial and lateral boundary conditions of meteorological forcing were provided by 6 h the National Center for Environmental Prediction final analysis (NCEP/FNL) data on 1×1 grids (https://psl.noaa.gov/data/). The chemical initial and boundary conditions were prepared using the mozbc utility tool based on the output of Model for Ozone and Related Chemical Tracers (MOZART) results acquired from the National Center for Atmospheric Research (NCAR) (https://www.acom.ucar.edu/wrf-chem/mozart.shtml). We adopted the Morrison-2-moment (Gustafson Jr et al., 2007), the Rapid Radiative Transfer Model (RRTMG) (Iacono et al., 2008; Mlawer et al., 1997), the revised MM5 (Paulson, 1970), the unified Noah (Chen and Dudhia, 2001), the GOCART (Ginoux et al., 2001), and the Yonsei University (YSU) schemes in this study. The simulation runs from January to December 2017, with the first week of January as a spin-up.

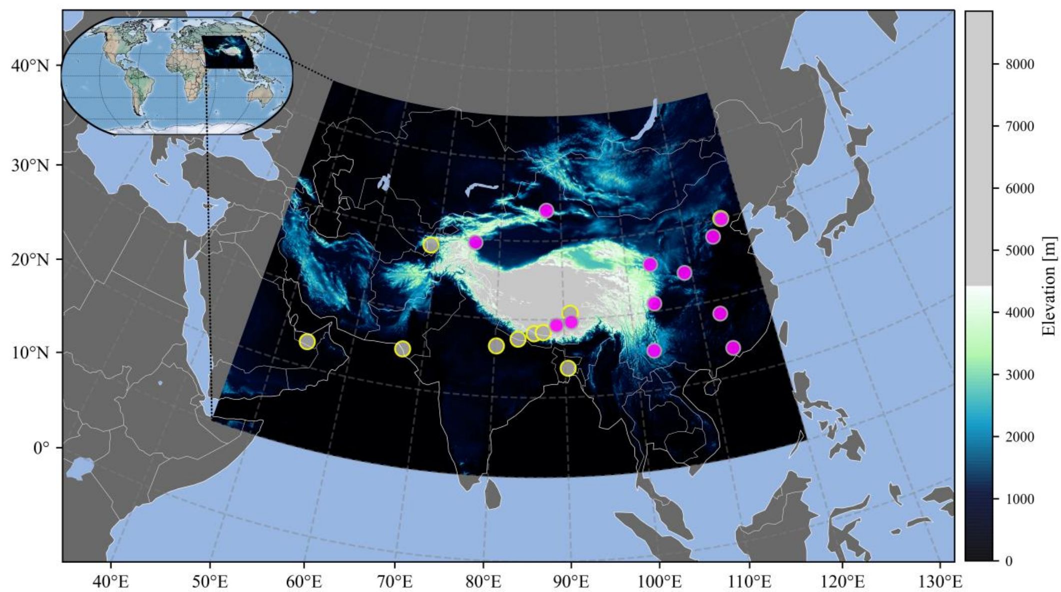

Figure 1. The research domain (dark blue shade) covering the Pan-Tibetan Plateau (PTP) region, with elevation shown in color code. The magenta and gray circular dots illustrate the location of PM (PM2.5 and PM10) and the AERONET stations, respectively for which data is used for the model validation.

https://doi.org/10.5194/acp-2022-199
Preprint. Discussion started: 11 April 2022

2.2. IPART module

IPART is a python module embedded with a new detection algorithm for tracking atmospheric rivers (AR) (Xu et al., 2020). However, in the present study, we utilized this module for extending the AR concept to aerosols considering the zonal and meridian long-range impact on air quality and extremes. To quantify IAT, we leverage the Modern-Era Retrospective analysis for Research and Applications (MERRA-2) assimilated product (Randles et al., 2017) with IPART. Such 2D single-level aerosols diagnostic dataset comes with 0.5°× 0.625° horizontal resolution. The data field is time-stamped with the central time of an hour starting from 00:30 to 23:30 UTC. Total IAT calculated based on the approaches defined by Xu et al. (2020) and Chakraborty et al. (2021) using the following formula.

$$\mathrm{IAT_n} = \sqrt{(\mathrm{IATU})_n{}^2 + (\mathrm{IATV})_n{}^2}$$

Here, n denotes each of the aerosol species treated, whereas U and V indicate corresponding zonal and meridional components of vertically integrated aerosol mass fluxes. We selected U and V components of each species namely BC, OC, and dust.

2.3. HYSPLIT model

To investigate the transport pathways and further provide evidence of the source-sink footprint of different pollutants. We calculated the seven-day back-trajectories (forward and backward in time) using the HYSPLIT model. Trajectories were initialized at 100 m above ground level for the 6 h interval (UTC, 00:00, 06:00, 12:00, and 18:00) at Langtang (28.21° N, 85.61° E; 4900 m a.s.l) in the southern slope of the Himalaya considering it as the transition point between polluted South Asia and background region (i.e, Tibetan Plateau or the Himalaya). The model was run for the entire year using gridded meteorological reanalysis dataset Global Data Assimilation System (GDAS, 1° spatial resolution) (https://www.ready.noaa.gov/gdas1.php).

2.4. Emission, observation, and reanalysis datasets

The anthropogenic emissions are obtained from Emission Database for Global Atmospheric Research and Hemisphere Transport of Air Pollution (EDGAR-HTAP, v2.2) which has been compiled using regional emissions grid maps for BC, OC, $PM_{2.5}$, PM_{10}, CH_4, SO_2, CO, NO_X, and NH_3 from different emissions sectors like industry, residential, agriculture, power, transportation, aviation, and shipping at 0.1°×0.1° (Janssens-Maenhout et al., 2015). Similarly, the

https://doi.org/10.5194/acp-2022-199
Preprint. Discussion started: 11 April 2022

biogenic emissions are prepared from the Model of Emission of Gases and Aerosol from Nature (MEGAN) (Guenther et al., 2006). Additionally, biomass burning emissions are obtained from the Fire Inventory NCAR (FINN) from the National Center for Atmospheric Research (NCAR) with hourly temporal resolution and 1 km horizontal resolution (Wiedinmyer et al., 2011).

To examine the model simulated vs. surface concentrations of $PM_{2.5}$ and PM_{10}, we obtained the observational data from the China Environmental Monitoring Stations accessed via (https://quotsoft.net/air/#archive). The daily average data from eight-station in mainland China were used to validate against model simulation.

For comparison, we also obtained the Aerosol Robotic Network (AERONET) (https://aeronet.gsfc.nasa.gov/) Level 2 AOD (aerosol optical depth) data at the locations namely Beijing (40.00°E, 116.38°N) in China, QOMS (28.37°E, 86.95°N, and Nam Co (30.77°E, 90.96°N) in Tibet (China), Langtang (28.21°E, 85.61°N) and Lumbini (27.49°E, 83.28°N) in Nepal, Dushanbe (38.55°E, 68.86°N) in Tajikistan, Mezaira (23.15°E, 53.78°N) in UAE, Dhaka (23.73°E, 90.40°N) in Bangladesh, Kanpur (26.51°E, 80.23°N) in India, Karachi (24.87°E, 67.03°N) in Pakistan. Karachi, Kanpur, Lumbini, and Dhaka are located in IGP. Level 2.0 data comes with cloud-screened and assured quality (with uncertainty range 0.01-0.02) but lack in consistency opted further treatment, which we have constrained by Level 1 data in our study. More details about calibration, data processing, instrumentation, accuracy assessment, and uncertainty are mentioned elsewhere (Eck et al., 1999; Holben et al., 1998; Dubovik et al., 2000).

The Copernicus Atmospheric Monitoring Service (CAMS) AOD was obtained from (https://ads.atmosphere.copernicus.eu/) which is the fourth generation Atmospheric Composition Reanalysis (EAC4) (Inness et al., 2019). The Visible Infrared Imaging Radiometer Suite (VIIRS) AOD was obtained via (https://ladsweb.modaps.eosdis.nasa.gov/). Additionally, MERRA-2 AOD and dust were obtained from Goddard Earth Sciences Data and Information Services Center (GES DISC, https://disc.gsfc.nasa.gov/) which have $0.25^{\circ} \times 0.25^{\circ}$ spatial resolution.

2. 3. Results and discussion

3.1. Comparative assessment of $PM_{2.5}$, PM_{10}, and AOD

To provide an insight into the model reproducibility here we strengthen our study by performing a comprehensive assessment by comparing model outputs with observations for selected pollutants. In doing so, we have shown PM_{10} and $PM_{2.5}$ concentrations in 2017 from measurements and corresponding WRF-Chem simulation at eight locations over mainland China

https://doi.org/10.5194/acp-2022-199
Preprint. Discussion started: 11 April 2022

in Figure 2. Amongst the selected sites, measured annual mean PM_{10} shows low values in background sites [Shigatse (41 µg m^{-3})] whereas higher concentrations were recorded in urban locations [e.g., Shijiazhuang (149 µg m^{-3}), Xi'an (112.4 µg m^{-3}), and Beijing (98 µg m^{-3})]. The $PM_{2.5}$ concentrations hold the same patterns as in the case of PM_{10}, relatively low concentrations were observed in a pristine location like Shigatse (18.3 µg m^{-3}) and higher in Shijiazhuang (86.1 µg m^{-3}), Xi'an (66.5 µg m^{-3}) and Beijing (62.6 µg m^{-3}). Model overestimated $PM_{2.5}$ with a mean bias (MB) in Shijiazhuang (51.9 µg m^{-3}), Changsha (170.1 µg m^{-3}), Beijing (49 µg m^{-3}), and Kunming (22.9 µg m^{-3}) whereas underestimated (with MB) in Xi'an (-93.6 µg m^{-3}), Urumqi (-61.1 µg m^{-3}), Shigatse (-34.2 µg m^{-3}) and Lanzhou (-36.3 µg m^{-3}). The frequency of episodic spikes densely occurs during winter and before the onset of monsoon (Figure 2), however, the model is unable to reproduce these peaks. In general, the model captured the temporal variations of particulate matter concentrations fairly well. The R^2 values indicated that the model reproduced the PM_{10} and $PM_{2.5}$ at an acceptable level for all stations except in Lanzhou (R^2 = 0.40) and Kunming (R^2 = 0.36) for PM_{10}. The bias could be jointly affected by unaccounted factors, such as meteorological fluctuations that the model was unable to capture (Zhang et al., 2016; Ding et al., 2019), anthropogenic and natural emissions (Ukhov et al., 2020b; Cai et al., 2017), and geography (Wang et al., 2018a; Zhao et al., 2020b).

In response to the strict government clean air action plan, a significant reduction of PM_{10} and $PM_{2.5}$ over China has been reported (Ding et al., 2019; Zhao et al., 2020b; Uno et al., 2020; Kang et al., 2019) however PM_{10} and $PM_{2.5}$ values are much higher than the guideline values of the World Health Organization (WHO) and national ambient air quality standard, China. As shown in Figure 2, the daily mean PM concentrations at all locations never drop below the WHO limit of PM_{10} (50 µg m^{-3}) and $PM_{2.5}$ (25 µg m^{-3}) except for a few occasions. During episodic events, the WHO and China limits for PM10 and PM2.5 were exceeded by a factor of 10 and 3 respectively, which is a matter of concern to be considered while formulating air pollution abatement policies and actions plans.

https://doi.org/10.5194/acp-2022-199
Preprint. Discussion started: 11 April 2022

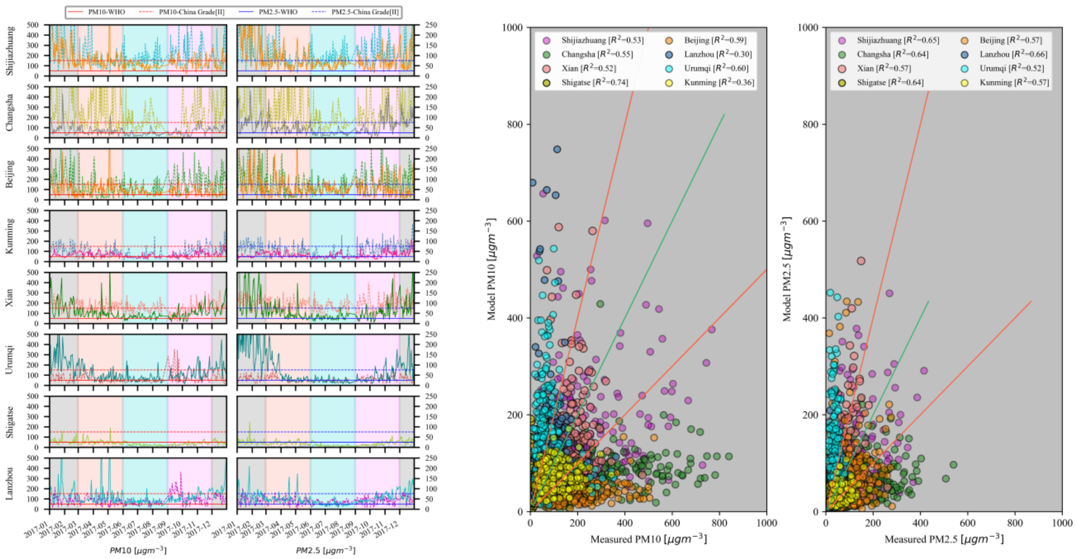

Figure 2. Daily PM10 and PM2.5 surface mass concentration for respective given locations from the observations and the corresponding WRF-Chem simulations for the simulation period. For each panel, the dashed and solid line corresponds to model and observation data whereas the horizontal dashed and the solid line indicates the air quality guideline values of WHO and China. From left to right, different color in the background represents the winter, spring summer, and autumn seasons. Scatter plot showing model vs. observation PM10 and PM2.5. Different dots colors represent the location-wise data. Solid straight lines are (2:1) - upper orange (1:1) - green and (2:1) - lower orange lines. The correlation coefficient values for each location are shown in the above figure. Other statistical metrics are given in Table S1.

AOD, an aerosol proxy, from the background and polluted stations was utilized for model validation. Figure 3 (first and second) shows a collocated time series plot for the observation, reanalysis, and modeled AOD whereas the Taylor diagram in the third column illustrated the seasonal mean statistical metrics for the model versus CAMS, MERRA-2, and VIIRS respectively. The AOD values correspond to urban than background locations. For all considered AERONET stations, the statistical score provided in Table 2s illustrated that the ground-based AOD satisfactory correlated with CAMS and MERRA-2 than WRF-Chem output. It is worth mentioning here that Gueymard and Yang (2020) study shows that MERRA-2 performs better than CAMS over most continents climates. The model vs. measured R^2 value was observed to be very low in Karachi (R^2 = 0.257, RMSE = 0.470) and Kanpur (R^2 = 0.278, RMSE = 0.470).

https://doi.org/10.5194/acp-2022-199
Preprint. Discussion started: 11 April 2022

Atmospheric Chemistry and Physics
Discussions

The observed mean AOD values in 2017 at AERONET sites in Beijing (0.44 ± 0.13), Dhaka (0.71 ± 0.14), Kanpur (0.69 ± 0.27), Mezaira (0.27 ± 0.08), QOMS (0.06 ± 0.05), Nam Co (0.06 ± 0.02), Lumbini (0.57 ± 0.20), Karachi (0.48 ± 0.16), and Dushanbe (0.30 ± 0.05) are comparable with other studies by Ramachandran et al. (2020a) from IGP locations, Pokharel et al. (2019) from Nam Co and Qoms, Rupakheti et al. (2018) from Lumbini, Rai et al. (2019) from Langtang, and Rupakheti et al. (2020) from Dushanbe. In the present study, the simulated AOD values are in line with previous findings. However, intrinsic uncertainty could be associated with the model resolution, emission data, meteorological influence, and data availability during the study period.

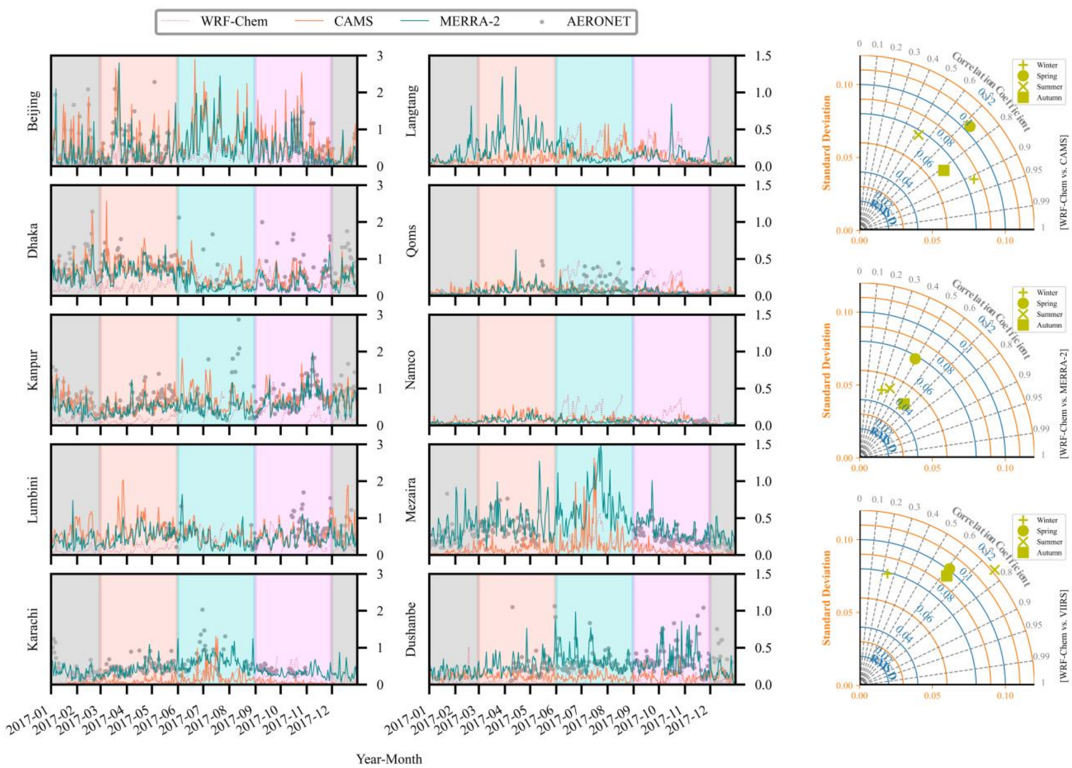

Figure 3. Time series of daily average AOD for the year 2017 (January-December) at ten AERONET sites for WRF-Chem (dashed magenta), CAMS (solid yellow), MERRA-2 (solid tan), and AERONET (circle grey). The first and second column shows the AERONET AOD with reanalysis data and WRF-Chem results for urban and background locations respectively. In the

https://doi.org/10.5194/acp-2022-199
Preprint. Discussion started: 11 April 2022

last column, the Taylor diagram represents the seasonal statistical metrics of WRF-Chem simulation data against VIIRS, MERRA-2, and CAMS data.

3. 3.2. Spatio-temporal seasonal aerosols and AOD variation and meteorological influence

The changes in atmospheric dynamics and meteorological conditions besides the emissions can change aerosol concentrations over the PTP region highlighting the need for studies on meteorological influence on spatiotemporal distributions of aerosols. Hence, exploiting model aerosol diagnostic output together with meteorological parameters here we unraveled the effects of such meteorological conditions on the spatiotemporal distribution of aerosol. For $PM_{2.5}$, PM_{10}, and OC three major hotspots with intense anthropogenic emissions were identified namely IGP, Sichuan Basin, and East China. In contrast, heavy dust concentrations are laden over Saudi Arabia, Central Asia, Taklamakan Desert, Gobi Desert, and Thar Desert (Figure 3, last column). Figure 4 shows clear seasonal variability with winter high and summer low concentrations for all aerosol species. In winter, aerosol concentrations were estimated maximum in the range 75-125 µg m^{-3} ($PM_{2.5}$), 100-200 µg m^{-3} (PM_{10}), 15-30 µg m^{-3} (OC) over South Asia and East China. During spring, aerosols concentrations were found to be relatively lower than winter ($PM_{2.5}$: 60-100 µg m^{-3}, PM_{10}: 25-125 µg m^{-3}, OC: 10-25 µg m^{-3}) reaching to lowest levels during summer ($PM_{2.5}$:15-70 µg m^{-3}, PM_{10}: 25-110 µg m^{-3}, OC: 5-15 µg m^{-3}) but again rebound to higher concentrations during autumn ($PM_{2.5}$: 30-90 µg m^{-3}, PM_{10}: 20-150 µg m^{-3}, OC:15-20 µg m^{-3}).

For the $PM_{2.5}$, the results from our simulation are comparable with Ojha et al. (2020) over the IGP region and Zhang et al. (2019a) over Eastern China. The maximum dust concentrations were over the Arabian Peninsula with concentrations of 400-600 µg m^{-3}, followed by the Taklamakan and Gobi Desert (300-500 µg m^{-3}), Central Asia (200-400 µg m^{-3}), and Thar Desert (200-450 µg m^{-3}). Annually, higher concentrations of $PM_{2.5}$, PM_{10}, and OC were estimated over the SA than EC region. Such changing pattern of aerosols concentrations over the region is also reported in previous studies (Crippa et al., 2018; Ding et al., 2019; Uno et al., 2020; Kanaya et al., 2020; Zhao et al., 2020c). In contrary to $PM_{2.5}$ and PM_{10}, OC concentrations were estimated higher over SA than EC as the emissions from biomass burning contributed more OC over SA than Eastern China. As stated by Han et al. (2020), extremely strong biomass burning in SA, mostly in spring affects the BC and OC concentrations.

https://doi.org/10.5194/acp-2022-199
Preprint. Discussion started: 11 April 2022

Atmospheric Chemistry and Physics Discussions

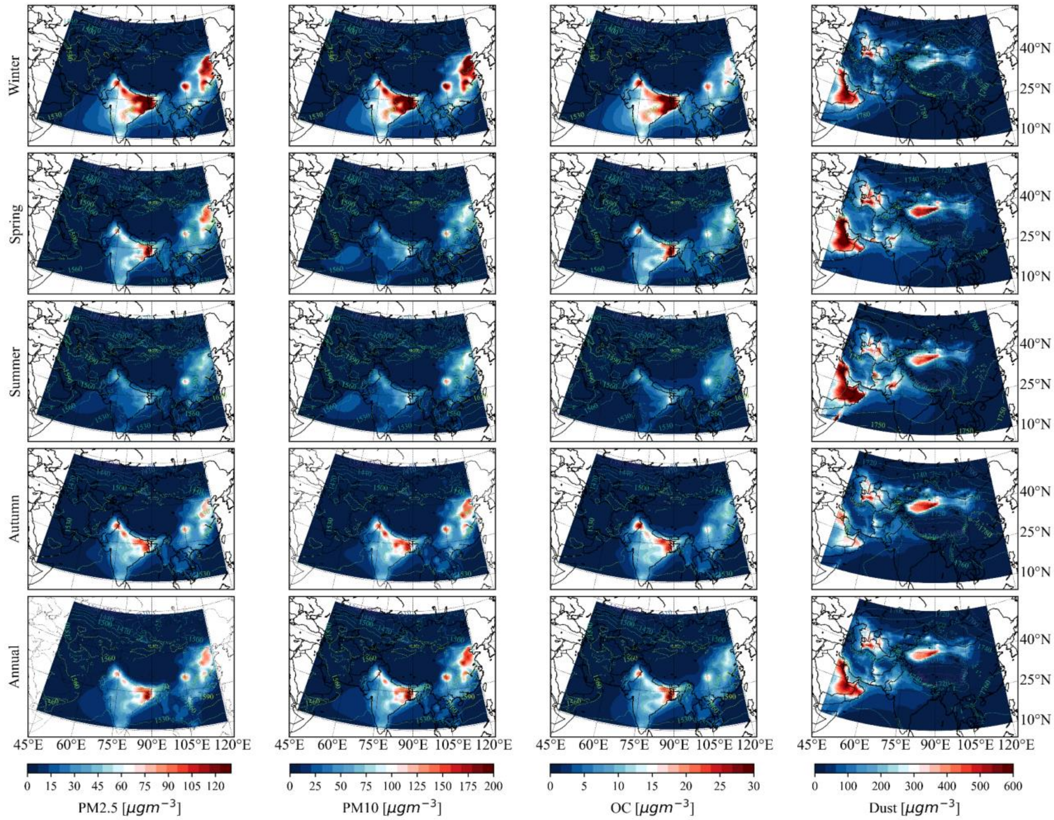

Figure 4. Seasonal spatio-temporal variation of aerosols ($PM_{2.5}$, PM_{10}, OC, and Dust). Color-coded contour line represents geopotential height at 850 hPa.

Regarding the AOD, as shown in Figure 5, a large spatial variation in AOD is observed over the PTP region. The higher AOD (>0.6) dominates over aerosols pool regions (Figure 4), i.e., IGP region, East India, Bangladesh, Sichuan Basin, East China, and dust rich regions like Saudi Arabia, Central Asia, Taklamakan Desert, Gobi Desert, and the Thar Desert. These regions are known to have heavy atmospheric aerosol loadings from anthropogenic emissions, wildfire emissions, biomass burning, and dust emissions (Gautam et al., 2011; Chen et al., 2013). On contrary but as expected, a relatively pristine region (i.e., TP, and the Himalayas) has lower AOD values as showed by WRF-Chem model, CAMS, MERRA-2, and VIIRS data throughout the simulation period. Our simulation results showed that the AOD was underestimated compared to the reanalysis data and satellite products. However, zonal mean statistical metrics (Figure 3, Taylor

https://doi.org/10.5194/acp-2022-199
Preprint. Discussion started: 11 April 2022

diagram) indicated that simulated results captured the general spatial-temporal patterns to some extent. Indeed, it should be noted that WRF-Chem masked out the general feature of AOD over Taklamakan Desert and Gobi Desert their surrounding regions. Over the Middle East and Arabian Peninsula, the AOD was underestimated by a factor of two. Such bias could be due to the choice of parameterization and the function used in the GOCART scheme where dust-dominated source regions are not well reproduced as the model is forced to run with a high spatial resolution (30 km). Uncertainty in AOD representation is in GOCART model described elsewhere (Parajuli et al., 2019; Ukhov et al., 2020a; Zhao et al., 2013). From a regional perspective, it is evident that the high magnitude of AOD is closely associated with the intense emission source regions including IGP, East China, and Sichuan Basin in all seasons that could have been resulted from rapid economic development including urbanization and industrial expansion. Another intrigued factor could be associated with biomass burning and anthropogenic emissions from highly populated regions. The distinct feature of high AOD over the Sichuan Basin could collectively be attributed to emission sources, topography, and meteorological conditions. As the mountain ridges inhibit the dispersion and transport of pollutants and stagnant meteorological conditions restrict the advection process that ultimately causes aerosol accumulation over a bowl-shaped basin which could result in higher AOD (Fan et al., 2020; Cao et al., 2020). Interestingly, high AOD also occurred over the Persian Gulf and the Arabian Sea. It could be linked with dust outflow from dust source regions in the Middle East in the West and the Thar Desert in the East (Figure 4). As stated by Nabavi et al. (2017) and Parajuli et al. (2019) the effect of the prevailing Shamal winds (strong northwesterly winds in the region) could result in dust storms, increased wind-blown dust, poor visibility, and worse air quality, and elevated AODs over the surrounding regions.

Irrespective of the seasonality, summer high AOD was found to be along the IGP region. A similar pattern with high AOD in summer and low in winter over IGP was reported in previous studies as well (Kulkarni et al., 2015; Ukhov et al., 2020a; Wang et al., 2020). In addition, a comprehensive study on multi-model evaluation by Pan et al. (2015) showed a clear indication of summer high and winter low over South Asia, with the maximum AOD stretching westward from East India to Kanpur in central IGP to Lahore in the western IGP and thus covering the entire IGP region.

https://doi.org/10.5194/acp-2022-199
Preprint. Discussion started: 11 April 2022

Atmospheric Chemistry and Physics Discussions

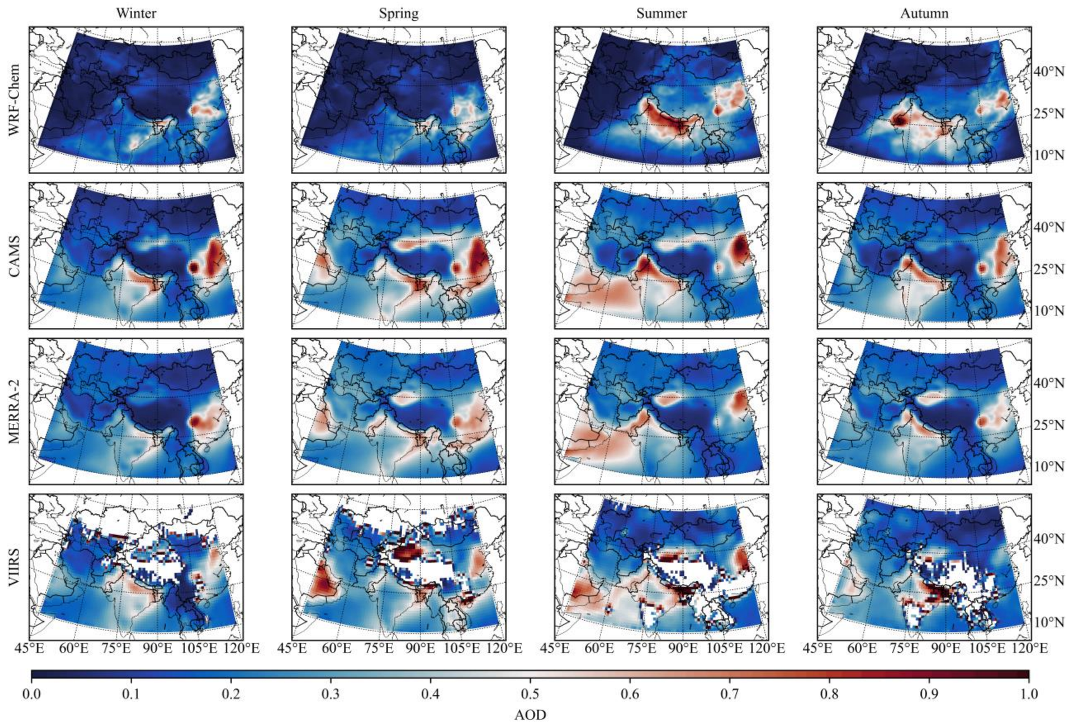

Figure 5. The seasonal mean AODs from the model simulation, reanalysis data, and satellite product for the simulation period (2017).

According to Ratnam et al. (2021) such enhanced AOD during summer is partly due to aerosol long-range transport through the low-level jet and tropical easterly jet that persists over the IGP region and due to a greater number of break spells. As stated by Pan et al. (2015), such AOD underestimation during winter over the IGP region might have been due to underlying multiple factors such as wintertime relative humidity (RH), proportionally higher presence of nitrate component in aerosols, inadequate representation of anthropogenic and biofuel emission, and open biomass burning activities. Feng et al. (2016) stated that the humidity bias results in the underestimation of AOD prediction over the South Asia region. Thus, summer high AOD could be modulated by enhanced temperature and RH that intensify hygroscopic growth of aerosols, consequently yielding high AOD (Alam et al., 2012; Altaratz et al., 2013). The biomass burning emissions, notably from forest fires and agro residue burning especially during the winter and spring seasons are a dominant source of pollutants and hence enhanced AODs over South Asia

https://doi.org/10.5194/acp-2022-199
Preprint. Discussion started: 11 April 2022

(Ramachandran et al., 2020b). Thus, it is believed that specific biomass burning events could not be captured well by the model subsequently led to an underestimation of AOD.

Emissions under unfavorable meteorological conditions for their dispersion cause air pollution episodes. Thus, apart from emissions, the variabilities in concentrations of air pollutants must depend on the effects of meteorological conditions which are of great significance in determining dispersion, atmospheric processing, and removal of air pollutants (Wang et al., 2018b). To showcase meteorological influence on the variation of aerosols here we have presented seasonal and annual meteorological parameters (i.e., total precipitation, planetary boundary layer height (PBLH), RH, and wind speed (Figure 6). The minimum aerosol concentrations were observed over IGP, East China, Bay of Bengal, and Arabian Peninsula (Figure 4) during summer coinciding with the maximum precipitation (Figure 6). The onset of the summer monsoon (rainy season) facilitates the wet removal process. Additionally, dynamical change in PBLH across South Asia and East China during summer further helps reduce aerosol concentrations near the surface significantly due to more efficient dispersion and transport of aerosols. A study by Zhao et al. (2020a) stated that the elevated PBLH facilitates vertical diffusion, leading to a reduction in $PM_{2.5}$ concentration over the Sichuan Basin. On contrary, aerosol concentrations typically increase during winter as it is favored by less precipitation, shallow PBLH (<100 m), low wind speed over extended periods, and additional seasonal sources such as brick production in South Asia (Mues et al, 2018). The seasonal simulated wind speed is relatively lower over the highly polluted region (i.e., South Asia) that inhibited the dispersion and transportation of aerosols. However, the high wind speed found over Arabian Peninsula that could drive dust storms and transport dust from such desert environments to downwind regions. Zhang et al. (2019b) study from East China and Ojha et al. (2020) study from South Asia also stated that haze events were associated with severe air stagnation conditions represented by low wind speed, low PBLH, temperature reduction, and high humidity.

3.3. Aerosols transport dynamics

The interaction between meteorological conditions and terrain exacerbates the severity of air pollution (Wang et al., 2018b). Under favorable circumstances, the aerosol particles are dispersed well and transported afar from source regions more efficiently. Thus, to examine such a mechanism and offer insight into the vertical distribution of aerosols here we have provided the

https://doi.org/10.5194/acp-2022-199
Preprint. Discussion started: 11 April 2022

cross-sectional zonal mean concentrations (Figure 7). The seasonal columnar profile exhibited that the maximum aerosols concentrations are limited within 1-2 km over South Asia and East China regions. The highest $PM_{2.5}$, PM_{10}, and OC concentrations are found near the surface with concentrations in the range of 50-100 µg m^{-3}, 70-100 µg m^{-3}, and 10-20 µg m^{-3}, respectively over the high emission source regions like IGP in the southern flank of the Himalayas and East China. Whereas, the higher extinction coefficient values correspond with the aerosol concentrations.

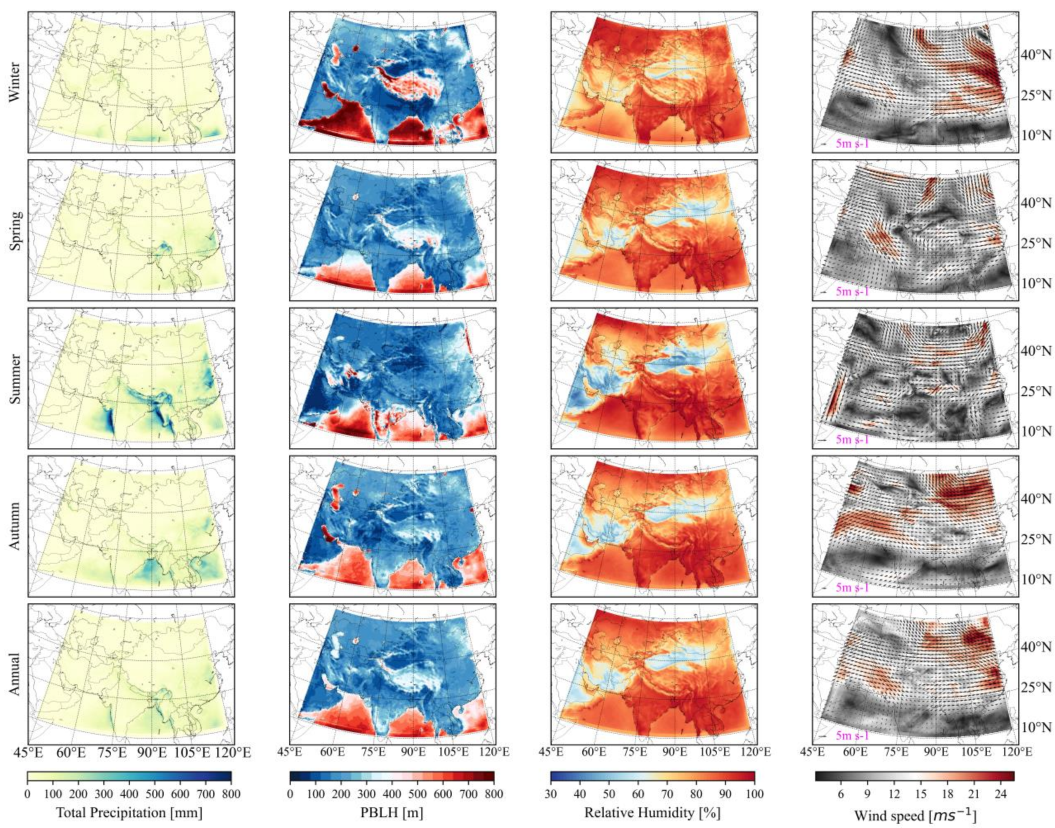

Figure 6. WRF-simulated seasonal and annual mean meteorological parameters. Wind speed interpolated at 500 hPa is indicated by color-code.

The maximum values of extinction coefficient were observed over aerosol-rich regions, i.e., South Asia and East China. However, noticeable higher values during winter and spring seasons over the HTP can be attributed to higher amounts of aerosols transported across the Himalayas to the Tibetan Plateau from upwind source regions in South Asia (Lüthi et al., 2015).

https://doi.org/10.5194/acp-2022-199
Preprint. Discussion started: 11 April 2022

Atmospheric Chemistry and Physics Discussions

During winter, higher aerosol concentrations are confined near the surface. However, aerosols start getting into higher elevations during spring. Such evident accumulation of aerosols was also observed by Zhang et al. (2020a). Apart from emissions, this could be attributed to weakening winter monsoon towards the end of the winter season, high humidity, an increase in the occurrence of calmer winds, reduction of wind shear of horizontal zonal winds, a decrease in precipitation, and low PBLH (Chen and Wang, 2015; Zhang et al., 2016).

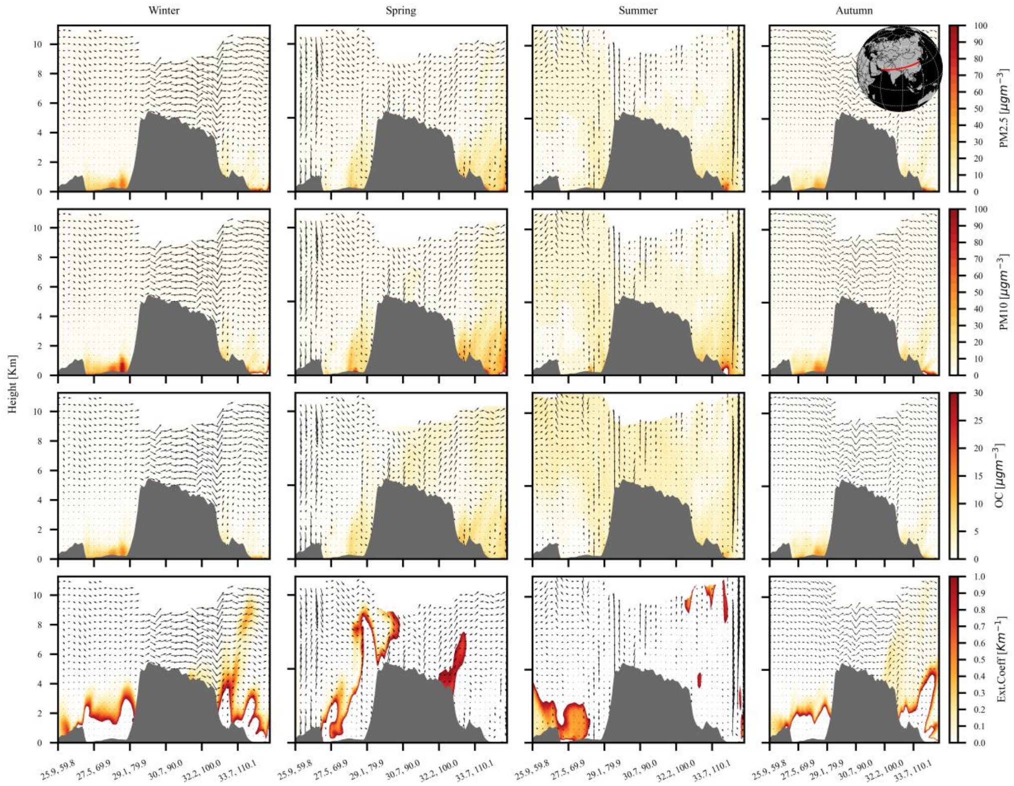

Figure 7. Seasonal cross-sectional columnar profile for PM2.5, PM10, OC, and aerosol extinction coefficient. The red line in the upper right corner shows the starting and endpoints of the cross-section transect. The filled gray color indicates terrain height and the arrow represents wind speed and wind direction.

In contrast, during summer the aerosol concentrations are elevated vertically as high as up to 10 km potentially driven by the deep convection and other summer monsoon activities. During summer in Figure 8, the higher density of air masses at 800-100 hPa in the Himalayas are received

https://doi.org/10.5194/acp-2022-199
Preprint. Discussion started: 11 April 2022

from the Bay of Bengal and Arabian Peninsula which further moved forward beyond the Himalayas and TP at 200-400 hPa. Such elevation differentiates air masses that could carry aerosol species from the surface to the different atmospheric layers. Bian et al. (2020) stated that convective overshooting events are also an efficient mechanism to transport the aerosols to the upper troposphere and lower stratosphere (UTLS) within the Asian Summer monsoon anticyclone. According to Zhao et al. (2017), the BC transport from South Asia to the TP during the summer monsoon was found to be strongly dependent on cyclonic activities and convergent airflows which significantly increased the BC in the TP. Whereas, Rai et al. (2022) stated that the role of different wind regime plays a crucial for the BC transportation that is even injected into UTLS region. As autumn approaches, the summer monsoon withdrawal process continues thereby weakening the convection process, which ultimately reduced the vertical aerosols concentrations.

Further, to investigate the aerosol transport mechanisms and pathways here we traced back air mass trajectories and assessed their forward trajectories, including through a clusters analysis (Figure 8). Except for the summer season, westerlies are a predominant wind received in the Himalayas (at Langtang) which moved forward (mostly eastward) to the Tibetan Plateau and East China. The clusters analysis indicated that the higher percentage of air masses traversed long distances over land (22% as far back as the Middle East and Central Asia and 30% confined mostly within South Asia) in long and dry winter and spring seasons that potentially transported higher aerosol concentrations from upwind intense source regions through long-range transport mechanism. On the other hand, the Bay of Bengal is the main source of air masses (mostly carrying heavy amounts of moisture) during summer that could lower aerosol concentrations at the surface through the wet scavenging process. However, such air masses could also inject pollution into the higher layers through deep convection and orographic lifting processes over the Himalayan region (Pan et al., 2015; Bian et al., 2020; Zhang et al., 2015b).

Previously, numerous studies have explored and documented the characteristics and mechanisms of aerosol transport over the HTP region (Han et al., 2020; Kopacz et al., 2011; Lüthi et al., 2015; Yang et al., 2018; Zhang et al., 2015a). Despite these findings, the current understanding of aerosol transport mechanisms and pathways, particularly its seasonal extremes is yet to be explored and advanced. Over the period, there has also been significant growth in studies related to water vapor transport that was termed as an atmospheric river (AR) (Neiman et al., 2011; Ralph et al., 2017; Guan and Waliser, 2015). Further, Chakraborty et al. (2021) extended the AR

https://doi.org/10.5194/acp-2022-199
Preprint. Discussion started: 11 April 2022

concept in terms of aerosol atmosphere river (AAR). Voss et al. (2020) investigated the dynamic association between dust and AR. The integrated aerosol transport (IAT) studies over the PTP region are rather recent. Therefore, here we leverage recent advances in IAT detection algorithm (Xu et al., 2020) to MERRA-2 dataset (Gelaro et al., 2017) to investigate spatiotemporal IAT distribution and potential association with the meteorology of the region.

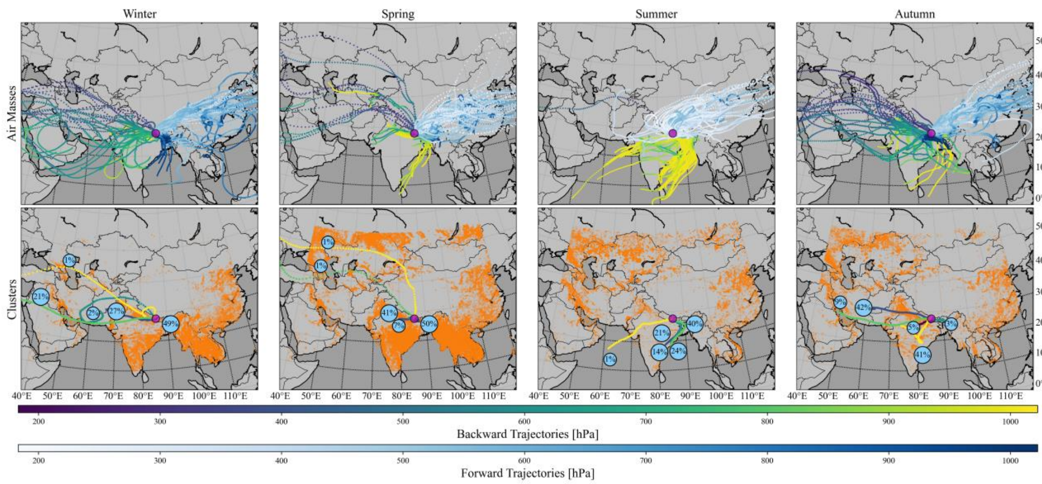

Figure 8. Seven-day seasonal backward/forward air mass trajectories and air mass clusters at Langtang (Nepal) for the year 2017 were generated by the HYSPLIT model. The yellow dotted color in the background represents the distribution of fire spot events that occurred in 2017. The fire data was obtained from the Suomi National Polar-Orbiting Partnership (Suomi NPP) satellite platform, which was acquired by the Visible Infrared Imaging Radiometer Suite (VIIRS).

During winter, BC_IAT showed a bipolar spatial distribution having one maximum over IGP in South Asia and another maximum over North China Plain (NCP) in East Asia, with the maximum BC_IAT of 2-2.5 × 10^{-5} kg m^{-1} s^{-1}. During the spring season, the BC_IAT pattern shifts eastwards, particularly the South Asian BC-IAP extending to northern Southeast Asia and south East Asia. The weakest BC_IAT was observed over both IGP (~ 1× 10^{-5} kg m^{-1} s^{-1}) and EC (1.5× 10^{-5} kg m^{-1} s^{-1}) during summer. Nevertheless, during autumn BC_IAT rebounded to its maximum of about 1-2 × 10^{-5} kg m^{-1} s^{-1} over IGP and 1.5-2 × 10^{-5} kg m^{-1} s^{-1} over EC. A similar spatiotemporal pattern has been observed for the OC_IAT. During winter, the IGP region had higher OC_IAT (8-10 × 10^{-5} kg m^{-1} s^{-1}) than the rest of the region. In spring, the OC_IAT pattern shifted toward East Asia along 90°E-120°E covering a large swath of northern Southeast Asia with very high OC_IAT (Figure 9). A clear picture of OC_IAT spring anomaly could be seen over East Asia (Figure 10),

https://doi.org/10.5194/acp-2022-199
Preprint. Discussion started: 11 April 2022

with the extreme reaching a maximum ~5 folds higher than the annual average (Figure 10). This could be explained by the contribution from the biomass burning emission. During spring, the fire events are maximum over Asia (Figure 8, spring). It can be thus inferred that OC_IAT contributed significantly to increasing aerosol extinction coefficient even over the HTP region (Figure 7). Chakraborty et al. (2021) mentioned that higher population regions like China and India are associated with BC and OC AAR that transport BC and OC aerosols either in the direction of the trade winds in tropics or westerlies in the multitude. Unlike BC_IAT and OC_IAT, a contrasting spatial distribution for Dust_IAT was found with a maximum over arid land and deserts including AP, PG, CA, TD, Gobi Desert, and the Thar Desert. Seasonally, the highest Dust_IAT (200-280 × 10^{-5} kg m^{-1} s^{-1}) is seen during summer over part of Saudi Arabia, CA, PG, and IGP. Chakraborty et al. (2021) found the largest Dust_IAT over the Middle East, Central Asia, and East China regions (~30 × 10^{-3} kg m^{-1} s^{-1}). Both simulation and other datasets revealed that summer high AOD over IGP (Figure 5). Thus, this could be possibly due to the response of high Dust_IAT from the neighboring regions under favorable meteorological conditions. High dust concentrations were found over Arabian Peninsula with the swatch of high dust concentrations extending over the IGP region during winter. However, on a global scale, Chakraborty et al. (2021) revealed that the AAR is responsible for transporting more than 40 % of the total IAT over tropical and mid-latitude regions.

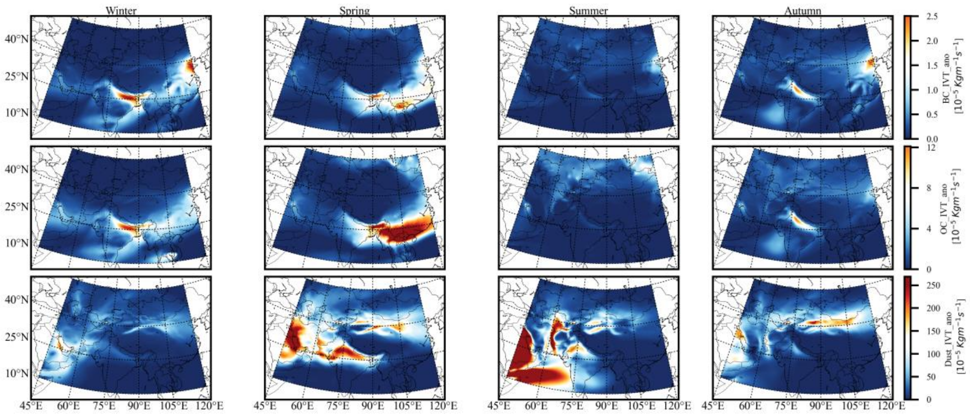

Figure 9. Seasonal integrated aerosol transport (IAT) for the BC, OC, and Dust for the year 2017 over the study region.

https://doi.org/10.5194/acp-2022-199
Preprint. Discussion started: 11 April 2022

Aerosol concentrations and distribution are complex processes governed by emissions, meteorological conditions, and land-atmosphere interactions. Except for emissions, the meteorology of a region is one of the prominent aerosol-modulating factors for aerosol transport and dispersion. Therefore, here we investigate the relationship of IAT with precipitation and wind speed (Figure 11). The strong negative correlation found over the BC and OC emission source regions (i.e., SA and EC) indicated that the precipitation affects the IAT significantly, as higher precipitation is likely to lower the IAT through the wet scavenging of aerosols. On contrary, a positive correlation with precipitation was found over Central Asia and Mongolia where emission is relatively low. Interestingly, the relationship of Dust_IAT with wind speed was opposite to that between IAT and precipitation.

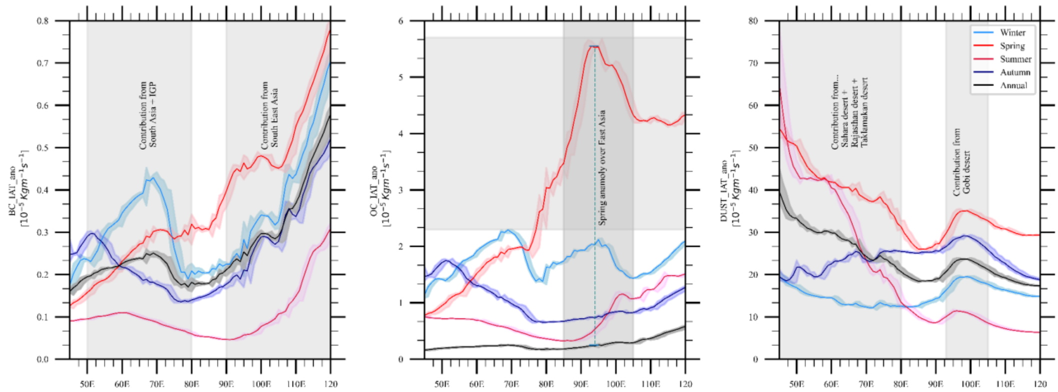

Figure 10. Seasonal-annual zonal mean of integrated aerosol transport (IAT) of BC, OC, and dust for the year 2017. The solid line indicated the meanwhile shaded identical color represent the ±1σ.

Contrary to precipitation, a positive correlation between wind and BC_IAT and OC_IAT were found over the emission source regions (Figure 11, (d, e)). The wind, one of the prominent meteorological drivers plays a crucial role in aerosols transport. The higher the wind speed the more BC and OC carried throughout the atmospheric column. Whereas, Voss et al. (2020) found that the dusty AR occurs when strong winds carry dust from Asia across the Pacific. Thus, it can be inferred that the different meteorological parameters and atmospheric dynamics can offset the benefits availed from a reduction in anthropogenic emissions (Ojha et al., 2020).

https://doi.org/10.5194/acp-2022-199
Preprint. Discussion started: 11 April 2022

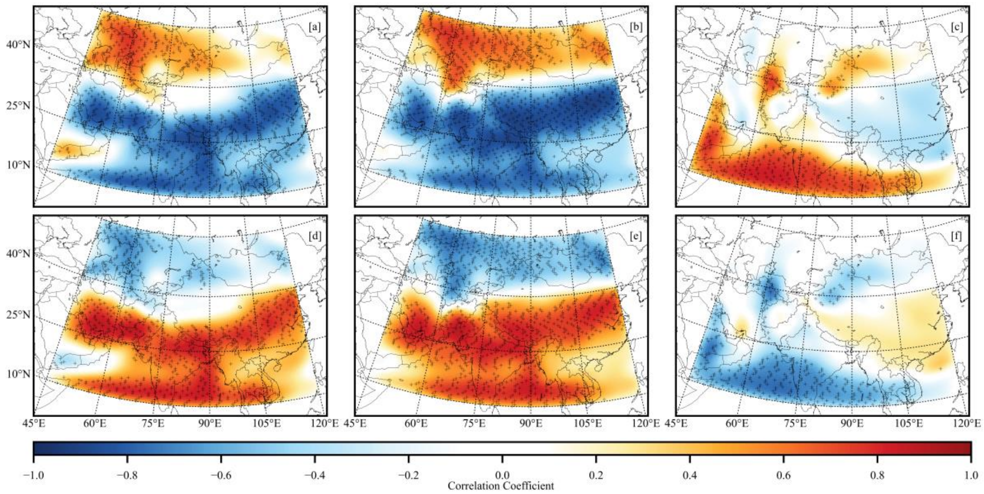

Figure 11. The relationship of BC_IAT, OC_IAT, and Dust_IAT with precipitation (a, b, c) and wind speed (d, e, f), respectively. Plus (+) symbol represents that passed the significant test with p <0.1.

Conclusions

This study reports the quantification of seasonal aerosol concentrations, investigation in transport dynamics, and meteorological influence over the PTP region by leveraging multi-sensors satellite, reanalysis dataset, and atmospheric model simulations. We have shown that the model can reproduce fairly well $PM_{2.5}$, PM_{10}, and AOD when compared with the observation data. However, we argued that the plausible biases could be due to unfavorable meteorological conditions, emissions, and the geographical setting of the region. Our finding showed that the aerosol concentrations exhibited clear seasonality with winter high and summer low. Such pronounced difference in aerosol concentrations could be favored by less precipitation, shallow PBLH, and low wind speed in winter. The higher AOD values correspond to aerosol concentrations. However, the higher AOD values during summer found over IGP could be explained by enhanced temperature and RH that support the hygroscopic growth of the aerosols. The seasonal columnar profile showed that the maximum aerosol concentrations are limited within 2 km above the surface over intense emission source regions like South Asia and East China.

https://doi.org/10.5194/acp-2022-199
Preprint. Discussion started: 11 April 2022

However, significant aerosol concentrations and aerosol extinction were also found over the HTP that could be attributed to injection through deep convection, orographic lifting, and long-range transport processes. From IAT calculation, BC and OC transport was confirmed predominantly during winter and spring over emission-rich regions whereas dust transport was originated in arid land and deserts and carried forward (eastward) by westerlies. Interestingly, a clear signature of OC transportation was noticed over Southeast Asia during spring that is directly linked with forest fire events in southern Asia. The spring anomaly of OC_IAT was found to be exceptionally high, five folds higher than the annual average. Additionally, we found that the effect of precipitation on IAT (higher precipitation - lower IAT) is opposite to that of wind speed on IAT (higher wind speed – higher IAT) over the emission source region. It is plausible that low wind speed caused stagnant aerosols but it higher wind speed facilitated transportation and dispersion of aerosols. Thus, we concluded that the distinctive aerosol seasonality and transport dynamics depend on the strength of emission source, process, and governing meteorological drivers. In the future, one could emphasize the critical role of the aerosol atmospheric river in air quality by considering more meteorological variables and societal impact, especially during extreme events.

Code and data availability

The AOD data used in this study are available at CAMS (https://ads.atmosphere.copernicus.eu/), MERRA-2 (https://disc.gsfc.nasa.gov/), and VIIRS (https://ladsweb.modaps.eosdis.nasa.gov/). The particulate matter data can be obtained via (https://quotsoft.net/air/#archive). The observational AOD can be accessed from (https://aeronet.gsfc.nasa.gov/). The model used in this study can be accessed from (https://ruc.noaa.gov/wrf/wrf-chem/). The other datasets and codes used in this study can be obtained from (https://github.com/mukeshraeee/Mukesh_ACP_Manuscript).

Author contributions

MR performed the model simulation, analysis, and prepared the figures. JY, XC, and YH contributed to data curation and formal analysis. SK, MR, DR, LT, and JY supervised writing, review, and editing. SK, JY, and MR conceptualized the paper. MR wrote the paper, with all the contributions from all co-authors. SK supervised the project.

https://doi.org/10.5194/acp-2022-199
Preprint. Discussion started: 11 April 2022

Atmospheric Chemistry and Physics Discussions

Competing interests

The contact author has declared that neither they nor their co-authors have any competing interests.

Acknowledgments

Mukesh Rai is supported by CAS-TWAS President's Fellowship for International Ph.D. students. Maheswar Rupakheti acknowledges the support provided by the IASS, which is funded by the German Federal Ministry for Education and Research (BMBF) and the Brandenburg Ministry for Science, Research, and Culture (MWFK). Dipesh Rupakheti is supported by The Startup Foundation for Introducing Talent of NUIST. We are grateful for the datasets and data archiving centers that supported this work and appreciate those who made our study possible, including CAMS, MERRA-2, AERONET, and VIIRS team. We also thank China Environmental Monitoring Station (https://quotsoft.net/air/#archive) for providing aerosols observation data. We are gratefully acknowledged for the python packages matplotlib for visualization (Hunter, 2007) and IPART for IAT calculation (Xu et al., 2020).

Financial support

This has been supported by the Strategic Priority Research Program of the Chinese Academy of Sciences, Pan-Third Pole Environment Study for a Green Silk Road (Pan-TPE) (XDA20040501), the National Natural Science Foundation of China (42071096), and the Key Research Program of the Chinese Academy of Sciences (QYZDJ-SSW-DQC039).

https://doi.org/10.5194/acp-2022-199
Preprint. Discussion started: 11 April 2022

Atmospheric Chemistry and Physics Discussions

References

Alam, K., Trautmann, T., Blaschke, T., and Majid, H.: Aerosol optical and radiative properties during summer and winter seasons over Lahore and Karachi, Atmospheric Environment, 50, 234-245, https://doi.org/10.1016/j.atmosenv.2011.12.027, 2012.

Altaratz, O., Bar-Or, R., Wollner, U., and Koren, I.: Relative humidity and its effect on aerosol optical depth in the vicinity of convective clouds, Environmental Research Letters, 8, 034025, 2013.

Bian, J., Li, D., Bai, Z., Li, Q., Lyu, D., and Zhou, X.: Transport of Asian surface pollutants to the global stratosphere from the Tibetan Plateau region during the Asian summer monsoon, National Science Review, 7, 516-533, https://doi.org/10.1093/nsr/nwaa005, 2020.

Cai, W., Li, K., Liao, H., Wang, H., and Wu, L.: Weather conditions conducive to Beijing severe haze more frequent under climate change, Nature Climate Change, 7, 257-262, https://doi.org/10.1038/nclimate3249, 2017.

Cao, B., Wang, X., Ning, G., Yuan, L., Jiang, M., Zhang, X., and Wang, S.: Factors influencing the boundary layer height and their relationship with air quality in the Sichuan Basin, China, Science of The Total Environment, 138584, https://doi.org/10.1016/j.scitotenv.2020.138584, 2020.

Carmichael, G. R., Adhikary, B., Kulkarni, S., D'Allura, A., Tang, Y., Streets, D., Zhang, Q., Bond, T. C., Ramanathan, V., Jamroensan, A., and Marrapu, P.: Asian Aerosols: Current and Year 2030 Distributions and Implications to Human Health and Regional Climate Change, Environmental Science & Technology, 43, 5811-5817, https://doi.org/10.1021/es8036803, 2009.

Chakraborty, S., Guan, B., Waliser, D. E., da Silva, A. M., Uluatam, S., and Hess, P.: Extending the Atmospheric River Concept to Aerosols: Climate and Air Quality Impacts, Geophysical Research Letters, 48, e2020GL091827, https://doi.org/10.1029/2020GL091827, 2021.

Charlson, R. J., Schwartz, S., Hales, J., Cess, R. D., Coakley, J. J., Hansen, J., and Hofmann, D.: Climate forcing by anthropogenic aerosols, Science, 255, 423-430, 10.1126/science.255.5043.423, 1992.

Chen, F. and Dudhia, J.: Coupling an Advanced Land Surface–Hydrology Model with the Penn State–NCAR MM5 Modeling System. Part I: Model Implementation and Sensitivity, Monthly Weather Review, 129, 569-585, 10.1175/1520-0493(2001)129<0569:CAALSH>2.0.CO;2, 2001.

Chen, H. and Wang, H.: Haze Days in North China and the associated atmospheric circulations based on daily visibility data from 1960 to 2012, Journal of Geophysical Research: Atmospheres, 120, 5895-5909, https://doi.org/10.1002/2015JD023225, 2015.

Chen, H., Li, Q., Kaufman, J. S., Wang, J., Copes, R., Su, Y., and Benmarhnia, T.: Effect of air quality alerts on human health: a regression discontinuity analysis in Toronto, Canada, The Lancet Planetary Health, 2, e19-e26, https://doi.org/10.1016/S2542-5196(17)30185-7, 2018.

Chen, S., Huang, J., Zhao, C., Qian, Y., Leung, L. R., and Yang, B.: Modeling the transport and radiative forcing of Taklimakan dust over the Tibetan Plateau: A case study in the summer of 2006, Journal of Geophysical Research: Atmospheres, 118, 797-812, https://doi.org/10.1002/jgrd.50122, 2013.

https://doi.org/10.5194/acp-2022-199
Preprint. Discussion started: 11 April 2022

Chen, S., Huang, J., Li, J., Jia, R., Jiang, N., Kang, L., Ma, X., and Xie, T.: Comparison of dust emissions, transport, and deposition between the Taklimakan Desert and Gobi Desert from 2007 to 2011, Science China Earth Sciences, 60, 1338-1355, 10.1007/s11430-016-9051-0, 2017.

Chinnam, N., Dey, S., Tripathi, S. N., and Sharma, M.: Dust events in Kanpur, northern India: Chemical evidence for source and implications to radiative forcing, Geophysical Research Letters, 33, https://doi.org/10.1029/2005GL025278, 2006.

Crippa, M., Guizzardi, D., Muntean, M., Schaaf, E., Dentener, F., van Aardenne, J. A., Monni, S., Doering, U., Olivier, J. G., and Pagliari, V.: Gridded emissions of air pollutants for the period 1970–2012 within EDGAR v4. 3.2, Earth Syst. Sci. Data, 10, 1987-2013, https://doi.org/10.5194/essd-10-1987-2018, 2018.

Dang, R. and Liao, H.: Severe winter haze days in the Beijing–Tianjin–Hebei region from 1985 to 2017 and the roles of anthropogenic emissions and meteorology, Atmosheric Chemistry and Physics 19, 10801-10816, https://doi.org/10.5194/acp-19-10801-2019, 2019.

Dhaka, S. K., Chetna, Kumar, V., Panwar, V., Dimri, A. P., Singh, N., Patra, P. K., Matsumi, Y., Takigawa, M., Nakayama, T., Yamaji, K., Kajino, M., Misra, P., and Hayashida, S.: PM2.5 diminution and haze events over Delhi during the COVID-19 lockdown period: an interplay between the baseline pollution and meteorology, Scientific Reports, 10, 13442, https://doi.org/10.1038/s41598-020-70179-8, 2020.

Ding, A., Huang, X., Nie, W., Chi, X., Xu, Z., Zheng, L., Xu, Z., Xie, Y., Qi, X., and Shen, Y.: Significant reduction of PM 2.5 in eastern China due to regional-scale emission control: evidence from SORPES in 2011–2018, Atmospheric Chemistry and Physics, 19, 11791-11801, 2019.

Ding, A. J., Huang, X., Nie, W., Sun, J. N., Kerminen, V.-M., Petäjä, T., Su, H., Cheng, Y. F., Yang, X.-Q., Wang, M. H., Chi, X. G., Wang, J. P., Virkkula, A., Guo, W. D., Yuan, J., Wang, S. Y., Zhang, R. J., Wu, Y. F., Song, Y., Zhu, T., Zilitinkevich, S., Kulmala, M., and Fu, C. B.: Enhanced haze pollution by black carbon in megacities in China, Geophysical Research Letters, 43, 2873-2879, https://doi.org/10.1002/2016GL067745, 2016.

Dubovik, O., Smirnov, A., Holben, B., King, M., Kaufman, Y., Eck, T., and Slutsker, I.: Accuracy assessments of aerosol optical properties retrieved from Aerosol Robotic Network (AERONET) Sun and sky radiance measurements, Journal of Geophysical Research: Atmospheres, 105, 9791-9806, https://doi.org/10.1029/2000JD900040, 2000.

Eck, T. F., Holben, B., Reid, J., Dubovik, O., Smirnov, A., O'neill, N., Slutsker, I., and Kinne, S.: Wavelength dependence of the optical depth of biomass burning, urban, and desert dust aerosols, Journal of Geophysical Research: Atmospheres, 104, 31333-31349, 1999.

Fan, H., Zhao, C., and Yang, Y.: A comprehensive analysis of the spatio-temporal variation of urban air pollution in China during 2014–2018, Atmospheric Environment, 220, 117066, 2020.

Feng, Y., Cadeddu, M., Kotamarthi, V., Renju, R., and Raju, C. S.: Humidity bias and effect on simulated aerosol optical properties during the Ganges Valley Experiment, Current Science, 93-100, 2016.

Gabrielli, P., Wegner, A., Sierra-Hernández, M. R., Beaudon, E., Davis, M., Barker, J. D., and Thompson, L. G.: Early atmospheric contamination on the top of the Himalayas since the onset of the European Industrial Revolution, Proceedings of the National Academy of Sciences, 117, 3967-3973, https://doi.org/10.1073/pnas.1910485117, 2020.

Gautam, R., Hsu, N., Tsay, S., Lau, K., Holben, B., Bell, S., Smirnov, A., Li, C., Hansell, R., and Ji, Q.: Accumulation of aerosols over the Indo-Gangetic plains and southern slopes of the Himalayas: distribution, properties and radiative effects during the 2009 pre-monsoon season, Atmospheric Chemistry and Physics, 11, 12841, https://doi.org/10.5194/acp-11-12841-2011, 2011.

Gelaro, R., McCarty, W., Suárez, M. J., Todling, R., Molod, A., Takacs, L., Randles, C. A., Darmenov, A., Bosilovich, M. G., Reichle, R., Wargan, K., Coy, L., Cullather, R., Draper, C., Akella, S., Buchard, V., Conaty, A., da Silva, A. M., Gu, W., Kim, G.-K., Koster, R., Lucchesi, R., Merkova, D., Nielsen, J. E., Partyka, G., Pawson, S., Putman, W., Rienecker, M., Schubert, S. D., Sienkiewicz, M., and Zhao, B.: The Modern-Era Retrospective Analysis for Research and Applications, Version 2 (MERRA-2), Journal of Climate, 30, 5419-5454, https://doi.org/10.1175/JCLI-D-16-0758.1, 2017.

Ghude, S. D., Chate, D. M., Jena, C., Beig, G., Kumar, R., Barth, M. C., Pfister, G. G., Fadnavis, S., and Pithani, P.: Premature mortality in India due to PM2.5 and ozone exposure, Geophysical Research Letters, 43, 4650-4658, https://doi.org/10.1002/2016GL068949, 2016.

Ginoux, P., Chin, M., Tegen, I., Prospero, J. M., Holben, B., Dubovik, O., and Lin, S. J.: Sources and distributions of dust aerosols simulated with the GOCART model, Journal of Geophysical Research: Atmospheres, 106, 20255-20273, https://doi.org/10.1029/2000JD000053, 2001.

Grell, G. A., Dudhia, J., and Stauffer, D. R.: A description of the fifth-generation Penn State/NCAR Mesoscale Model (MM5), http://dx.doi.org/10.5065/D60Z716B, 1994.

Guan, B. and Waliser, D. E.: Detection of atmospheric rivers: Evaluation and application of an algorithm for global studies, Journal of Geophysical Research: Atmospheres, 120, 12514-12535, https://doi.org/10.1002/2015JD024257, 2015.

Guenther, A., Karl, T., Harley, P., Wiedinmyer, C., Palmer, P., and Geron, C.: Estimates of global terrestrial isoprene emissions using MEGAN (Model of Emissions of Gases and Aerosols from Nature), 3181–3210, https://doi.org/10.5194/acp-6-3181-2006, 2006.

Gueymard, C. A. and Yang, D.: Worldwide validation of CAMS and MERRA-2 reanalysis aerosol optical depth products using 15 years of AERONET observations, Atmospheric Environment, 225, 117216, 2020.

Gui, K., Che, H., Wang, Y., Xia, X., Holben, B. N., Goloub, P., Cuevas-Agulló, E., Yao, W., Zheng, Y., Zhao, H., Li, L., and Zhang, X.: A global-scale analysis of the MISR Level-3 aerosol optical depth (AOD) product: Comparison with multi-platform AOD data sources, Atmospheric Pollution Research, 12, 101238, https://doi.org/10.1016/j.apr.2021.101238, 2021.

Gustafson Jr, W. I., Chapman, E. G., Ghan, S. J., Easter, R. C., and Fast, J. D.: Impact on modeled cloud characteristics due to simplified treatment of uniform cloud condensation nuclei during NEAQS 2004, Geophysical Research Letters, 34, 2007.

Han, H., Wu, Y., Liu, J., Zhao, T., Zhuang, B., Wang, H., Li, Y., Chen, H., Zhu, Y., Liu, H., Wang, Q., Li, S., Wang, T., Xie, M., and Li, M.: Impacts of atmospheric transport and biomass burning on the inter-annual variation in black carbon aerosols over the Tibetan Plateau, Atmosheric Chemistry and Physics, 20, 13591-13610, https://doi.org/10.5194/acp-20-13591-2020, 2020.

Haywood, J. and Boucher, O.: Estimates of the direct and indirect radiative forcing due to tropospheric aerosols: A review, Reviews of geophysics, 38, 513-543, https://doi.org/10.1029/1999RG000078, 2000.

https://doi.org/10.5194/acp-2022-199
Preprint. Discussion started: 11 April 2022

Atmospheric Chemistry and Physics Discussions

Holben, B. N., Eck, T. F., Slutsker, I. a., Tanre, D., Buis, J., Setzer, A., Vermote, E., Reagan, J. A., Kaufman, Y., and Nakajima, T.: AERONET—A federated instrument network and data archive for aerosol characterization, Remote sensing of environment, 66, 1-16, https://doi.org/10.1016/S0034-4257(98)00031-5, 1998.

Hong, C., Zhang, Q., Zhang, Y., Davis, S. J., Tong, D., Zheng, Y., Liu, Z., Guan, D., He, K., and Schellnhuber, H. J.: Impacts of climate change on future air quality and human health in China, Proceedings of the National Academy of Sciences, 116, 17193-17200, https://doi.org/10.1073/pnas.1812881116, 2019.

Huang, X., Wang, Z., and Ding, A.: Impact of Aerosol-PBL Interaction on Haze Pollution: Multiyear Observational Evidences in North China, Geophysical Research Letters, 45, 8596-8603, https://doi.org/10.1029/2018GL079239, 2018.

Huang, X., Huang, J., Ren, C., Wang, J., Wang, H., Wang, J., Yu, H., Chen, J., Gao, J., and Ding, A.: Chemical Boundary Layer and Its Impact on Air Pollution in Northern China, Environmental Science & Technology Letters, 7, 826-832,

https://doi.org/10.1021/acs.estlett.0c00755, 2020.

Hunter, J. D.: Matplotlib: A 2D Graphics Environment, Computing in Science & Engineering, 9, 90-95, 10.1109/MCSE.2007.55, 2007.

Iacono, M. J., Delamere, J. S., Mlawer, E. J., Shephard, M. W., Clough, S. A., and Collins, W. D.: Radiative forcing by long-lived greenhouse gases: Calculations with the AER radiative transfer models, Journal of Geophysical Research: Atmospheres, 113, https://doi.org/10.1029/2008JD009944, 2008.

Inness, A., Ades, M., Agusti-Panareda, A., Barré, J., Benedictow, A., Blechschmidt, A.-M., Dominguez, J., Engelen, R., Eskes, H., and Flemming, J.: The CAMS reanalysis of atmospheric composition, Atmospheric Chemistry and Physics, 19, 3515-3556, https://doi.org/10.5194/acp-19-3515-2019, 2019.

Islam, M. R., Jayarathne, T., Simpson, I. J., Werden, B., Maben, J., Gilbert, A., Praveen, P. S., Adhikari, S., Panday, A. K., Rupakheti, M., Blake, D. R., Yokelson, R. J., DeCarlo, P. F., Keene, W. C., and Stone, E. A.: Ambient air quality in the Kathmandu Valley, Nepal, during the pre-monsoon: concentrations and sources of particulate matter and trace gases, Atmosheric Chemistry and Physics, 20, 2927-2951, https://doi.org/10.5194/acp-20-2927-2020, 2020.

Janssens-Maenhout, G., Crippa, M., Guizzardi, D., Dentener, F., Muntean, M., Pouliot, G., Keating, T., Zhang, Q., Kurokawa, J., and Wankmüller, R.: HTAP_v2. 2: a mosaic of regional and global emission grid maps for 2008 and 2010 to study hemispheric transport of air pollution, Atmospheric Chemistry and Physics, 15, 11411-11432, https://doi.org/10.5194/acp-15-11411-2015, 2015.

Jena, C., Ghude, S. D., Kumar, R., Debnath, S., Govardhan, G., Soni, V. K., Kulkarni, S. H., Beig, G., Nanjundiah, R. S., and Rajeevan, M.: Performance of high resolution (400 m) PM2.5 forecast over Delhi, Scientific Reports, 11, 4104, https://doi.org/10.1038/s41598-021-83467-8, 2021.

Jerrett, M.: The death toll from air-pollution sources, Nature, 525, 330-331, https://doi.org/10.1038/525330a, 2015.

Kanaya, Y., Yamaji, K., Miyakawa, T., Taketani, F., Zhu, C., Choi, Y., Komazaki, Y., Ikeda, K., Kondo, Y., and Klimont, Z.: Rapid reduction in black carbon emissions from China: evidence from 2009–2019 observations on Fukue Island, Japan, Atmospheric Chemistry and Physics, 20, 6339-6356, https://doi.org/10.5194/acp-20-6339-2020, 2020.

Kang, S., Xu, Y., You, Q., Flügel, W.-A., Pepin, N., and Yao, T.: Review of climate and cryospheric change in the Tibetan Plateau, Environmental research letters, 5, 015101, https://doi.org/10.1088/1748-9326/5/1/015101, 2010.

Kang, S., Zhang, Q., Qian, Y., Ji, Z., Li, C., Cong, Z., Zhang, Y., Guo, J., Du, W., and Huang, J.: Linking atmospheric pollution to cryospheric change in the Third Pole region: current progress and future prospects, National Science Review, 6, 796-809, https://doi.org/10.1093/nsr/nwz031, 2019.

Kong, L., Tang, X., Zhu, J., Wang, Z., Li, J., Wu, H., Wu, Q., Chen, H., Zhu, L., Wang, W., Liu, B., Wang, Q., Chen, D., Pan, Y., Song, T., Li, F., Zheng, H., Jia, G., Lu, M., Wu, L., and Carmichael, G. R.: A 6-year-long (2013–2018) high-resolution air quality reanalysis dataset in China based on the assimilation of surface observations from CNEMC, Earth Syst. Sci. Data, 13, 529-570, https://doi.org/10.5194/essd-13-529-2021, 2021.

Kopacz, M., Mauzerall, D. L., Wang, J., Leibensperger, E., Henze, D., and Singh, K.: Origin and radiative forcing of black carbon transported to the Himalayas and Tibetan Plateau, Atmospheric Chemistry and Physics 2837–2852, https://doi.org/10.5194/acp-11-2837-2011, 2011.

Kulkarni, S., Sobhani, N., Miller-Schulze, J., Shafer, M., Schauer, J., Solomon, P., Saide, P., Spak, S., Cheng, Y., and Denier Van Der Gon, H.: Source sector and region contributions to BC and PM2. 5 in Central Asia, Atmospheric Chemistry and Physics 15, 1683–1705, https://doi.org/10.5194/acp-15-1683-2015, 2015.

Kumar, R., Barth, M. C., Pfister, G. G., Naja, M., and Brasseur, G. P.: WRF-Chem simulations of a typical pre-monsoon dust storm in northern India: influences on aerosol optical properties and radiation budget, Atmosheric Chemistry and Physics, 14, 2431-2446, 10.5194/acp-14-2431-2014, 2014.

Kumar, R., Barth, M., Nair, V., Pfister, G., Suresh Babu, S., Satheesh, S., Moorthy, K. K., Carmichael, G., Lu, Z., and Streets, D.: Sources of black carbon aerosols in South Asia and surrounding regions during the Integrated Campaign for Aerosols, Gases and Radiation Budget (ICARB), Atmospheric Chemistry and Physics 15, https://doi.org/10.5194/acp-14-2431-2014, 2015.

Kumar, R., Barth, M. C., Pfister, G. G., Delle Monache, L., Lamarque, J. F., Archer-Nicholls, S., Tilmes, S., Ghude, S. D., Wiedinmyer, C., Naja, M., and Walters, S.: How Will Air Quality Change in South Asia by 2050?, Journal of Geophysical Research: Atmospheres, 123, 1840-1864, https://doi.org/10.1002/2017JD027357, 2018.

Kumar, R., Ghude, S. D., Biswas, M., Jena, C., Alessandrini, S., Debnath, S., Kulkarni, S., Sperati, S., Soni, V. K., Nanjundiah, R. S., and Rajeevan, M.: Enhancing Accuracy of Air Quality and Temperature Forecasts During Paddy Crop Residue Burning Season in Delhi Via Chemical Data Assimilation, Journal of Geophysical Research: Atmospheres, 125, e2020JD033019, https://doi.org/10.1029/2020JD033019, 2020.

Lelieveld, J., Evans, J. S., Fnais, M., Giannadaki, D., and Pozzer, A.: The contribution of outdoor air pollution sources to premature mortality on a global scale, Nature, 525, 367-371, https://doi.org/10.1038/nature15371, 2015.

Li, J.: Pollution Trends in China from 2000 to 2017: A Multi-Sensor View from Space, Remote Sensing, 12, 208, https://doi.org/10.3390/rs12020208, 2020.

Li, K., Liao, H., Zhu, J., and Moch, J. M.: Implications of RCP emissions on future PM2.5 air quality and direct radiative forcing over China, Journal of Geophysical Research: Atmospheres, 121, 12,985-913,008, https://doi.org/10.1002/2016JD025623, 2016a.

Li, L. and Sokolik, I. N.: The Dust Direct Radiative Impact and Its Sensitivity to the Land Surface State and Key Minerals in the WRF-Chem-DuMo Model: A Case Study of Dust Storms in Central Asia, Journal of Geophysical Research: Atmospheres, 123, 4564-4582, https://doi.org/10.1029/2017JD027667, 2018.

Li, Z., Lau, W. K. M., Ramanathan, V., Wu, G., Ding, Y., Manoj, M. G., Liu, J., Qian, Y., Li, J., Zhou, T., Fan, J., Rosenfeld, D., Ming, Y., Wang, Y., Huang, J., Wang, B., Xu, X., Lee, S. S., Cribb, M., Zhang, F., Yang, X., Zhao, C., Takemura, T., Wang, K., Xia, X., Yin, Y., Zhang, H., Guo, J., Zhai, P. M., Sugimoto, N., Babu, S. S., and Brasseur, G. P.: Aerosol and monsoon climate interactions over Asia, Reviews of Geophysics, 54, 866-929, https://doi.org/10.1002/2015RG000500, 2016b.

Liu, S., Xing, J., Sahu, S. K., Liu, X., Liu, S., Jiang, Y., Zhang, H., Li, S., Ding, D., Chang, X., and Wang, S.: Wind-blown dust and its impacts on particulate matter pollution in northern China: current and future scenario, Environmental Research Letters, 2021.

Lu, Z., Streets, D. G., Zhang, Q., and Wang, S.: A novel back-trajectory analysis of the origin of black carbon transported to the Himalayas and Tibetan Plateau during 1996–2010, Geophysical Research Letters, 39, https://doi.org/10.1029/2011GL049903, 2012.

Lüthi, Z. L., Škerlak, B., Kim, S. W., Lauer, A., Mues, A., Rupakheti, M., and Kang, S.: Atmospheric brown clouds reach the Tibetan Plateau by crossing the Himalayas, Atmosheric Chemistry and Physics, 15, 6007-6021, https://doi.org/10.5194/acp-15-6007-2015, 2015.

Lv, Z., Wei, W., Cheng, S., Han, X., and Wang, X.: Meteorological characteristics within boundary layer and its influence on PM2.5 pollution in six cities of North China based on WRF-Chem, Atmospheric Environment, 228, 117417, https://doi.org/10.1016/j.atmosenv.2020.117417, 2020.

Manisalidis, I., Stavropoulou, E., Stavropoulos, A., and Bezirtzoglou, E.: Environmental and Health Impacts of Air Pollution: A Review, Frontiers in Public Health, 8, https://doi.org/10.3389/fpubh.2020.00014, 2020.

Menon, S., Hansen, J., Nazarenko, L., and Luo, Y.: Climate effects of black carbon aerosols in China and India, Science, 297, 2250-2253, 10.1126/science.1075159, 2002.

Ming, J., Cachier, H., Xiao, C., Qin, D., Kang, S., Hou, S., and Xu, J.: Black carbon record based on a shallow Himalayan ice core and its climatic implications, Atmosheric Chemistry and Physics, 8, 1343–1352, https://doi.org/10.5194/acp-8-1343-2008, 2008.

Mlawer, E. J., Taubman, S. J., Brown, P. D., Iacono, M. J., and Clough, S. A.: Radiative transfer for inhomogeneous atmospheres: RRTM, a validated correlated-k model for the longwave, Journal of Geophysical Research: Atmospheres, 102, 16663-16682, https://doi.org/10.1029/97JD00237, 1997.

Moorthy, K. K., Babu, S. S., and Satheesh, S.: Aerosol characteristics and radiative impacts over the Arabian Sea during the intermonsoon season: Results from ARMEX field campaign, Journal of Atmospheric Sciences, 62, 192-206, https://doi.org/10.1175/JAS-3378.1, 2005.

Nabavi, S. O., Haimberger, L., and Samimi, C.: Sensitivity of WRF-chem predictions to dust source function specification in West Asia, Aeolian Research, 24, 115-131, https://doi.org/10.1016/j.aeolia.2016.12.005, 2017.

Neiman, P. J., Schick, L. J., Ralph, F. M., Hughes, M., and Wick, G. A.: Flooding in Western Washington: The Connection to Atmospheric Rivers, Journal of Hydrometeorology, 12, 1337-1358, https://doi.org/10.1175/2011JHM1358.1, 2011.

Ojha, N., Sharma, A., Kumar, M., Girach, I., Ansari, T. U., Sharma, S. K., Singh, N., Pozzer, A., and Gunthe, S. S.: On the widespread enhancement in fine particulate matter across the Indo-Gangetic Plain towards winter, Scientific Reports, 10, 5862, https://doi.org/10.1038/s41598-020-62710-8, 2020.

Pan, X., Chin, M., Gautam, R., Bian, H., Kim, D., Colarco, P. R., Diehl, T. L., Takemura, T., Pozzoli, L., and Tsigaridis, K.: A multi-model evaluation of aerosols over South Asia: common problems and possible causes, Atmosheric Chemistry and Physics, 15, 5903–5928, https://doi.org/10.5194/acp-15-5903-2015, 2015.

Parajuli, S. P., Stenchikov, G. L., Ukhov, A., and Kim, H.: Dust Emission Modeling Using a New High-Resolution Dust Source Function in WRF-Chem With Implications for Air Quality, Journal of Geophysical Research: Atmospheres, 124, 10109-10133, https://doi.org/10.1029/2019JD030248, 2019.

Paulson, C. A.: The mathematical representation of wind speed and temperature profiles in the unstable atmospheric surface layer, Journal of Applied Meteorology, 9, 857-861, https://doi.org/10.1175/1520-0450(1970)009<0857:TMROWS>2.0.CO;2, 1970.

Pokharel, M., Guang, J., Liu, B., Kang, S., Ma, Y., Holben, B. N., Xia, X. a., Xin, J., Ram, K., and Rupakheti, D.: Aerosol properties over Tibetan Plateau from a decade of AERONET measurements: baseline, types, and influencing factors, Journal of Geophysical Research: Atmospheres, 124, 13357-13374, https://doi.org/10.1029/2019JD031293, 2019.

Putero, D., Cristofanelli, P., Marinoni, A., Adhikary, B., Duchi, R., Shrestha, S. D., Verza, G. P., Landi, T. C., Calzolari, F., Busetto, M., Agrillo, G., Biancofiore, F., Di Carlo, P., Panday, A. K., Rupakheti, M., and Bonasoni, P.: Seasonal variation of ozone and black carbon observed at Paknajol, an urban site in the Kathmandu Valley, Nepal, Atmosheric Chemistry and Physics, 15, 13957-13971, https://doi.org/10.5194/acp-15-13957-2015, 2015.

Rai, M., Kang, S., Yang, J., Chen, X., Hu, Y., and Rupakheti, D.: Tracing atmospheric anthropogenic black carbon and its potential radiative response over Pan-Third Pole region: a synoptic-scale analysis using WRF-Chem, Journal of Geophysical Research: Atmospheres, n/a, e2021JD035772, https://doi.org/10.1029/2021JD035772, 2022.

Rai, M., Mahapatra, P. S., Gul, C., Kayastha, R. B., Panday, A. K., and Puppala, S. P.: Aerosol Radiative Forcing Estimation over a Remote High-altitude Location (~4900 masl) near Yala Glacier, Nepal, Aerosol and Air Quality Research, 19, 1872-1891, https://doi.org/10.4209/aaqr.2018.09.0342 2019.

Ralph, F. M., Iacobellis, S. F., Neiman, P. J., Cordeira, J. M., Spackman, J. R., Waliser, D. E., Wick, G. A., White, A. B., and Fairall, C.: Dropsonde Observations of Total Integrated Water Vapor Transport within North Pacific Atmospheric Rivers, Journal of Hydrometeorology, 18, 2577-2596, https://doi.org/10.1175/JHM-D-17-0036.1, 2017.

Ramachandran, S., Rupakheti, M., and Lawrence, M. G.: Black carbon dominates the aerosol absorption over the Indo-Gangetic Plain and the Himalayan foothills, Environment International, 142, 105814, https://doi.org/10.1016/j.envint.2020.105814, 2020a.

Ramachandran, S., Rupakheti, M., and Lawrence, M. G.: Aerosol-induced atmospheric heating rate decreases over South and East Asia as a result of changing content and composition, Scientific Reports, 10, 20091, https://doi.org/10.1038/s41598-020-76936-z, 2020b.

Ramanathan, V., Crutzen, P., Kiehl, J., and Rosenfeld, D.: Aerosols, climate, and the hydrological cycle, science, 294, 2119-2124, 10.1126/science.1064034, 2001.

Ramanathan, V., Ramana, M. V., Roberts, G., Kim, D., Corrigan, C., Chung, C., and Winker, D.: Warming trends in Asia amplified by brown cloud solar absorption, Nature, 448, 575-578, https://doi.org/10.1038/nature06019, 2007.

Randles, C., Da Silva, A., Buchard, V., Colarco, P., Darmenov, A., Govindaraju, R., Smirnov, A., Holben, B., Ferrare, R., and Hair, J.: The MERRA-2 aerosol reanalysis, 1980 onward. Part I: System description and data assimilation evaluation, Journal of Climate, 30, 6823-6850, https://doi.org/10.1175/JCLI-D-16-0609.1, 2017.

Ratnam, M. V., Prasad, P., Raj, S. T. A., Raman, M. R., and Basha, G.: Changing patterns in aerosol vertical distribution over South and East Asia, Scientific Reports, 11, 308, https://doi.org/10.1038/s41598-020-79361-4, 2021.

Ravishankara, A. R., David, L. M., Pierce, J. R., and Venkataraman, C.: Outdoor air pollution in India is not only an urban problem, Proceedings of the National Academy of Sciences, 117, 28640-28644, 10.1073/pnas.2007236117, 2020.

Rupakheti, D., Rupakheti, M., Abdullaev, S. F., Yin, X., and Kang, S.: Columnar aerosol properties and radiative effects over Dushanbe, Tajikistan in Central Asia, Environmental Pollution, 114872, 2020.

Rupakheti, D., Kang, S., Rupakheti, M., Cong, Z., Tripathee, L., Panday, A. K., and Holben, B. N.: Observation of optical properties and sources of aerosols at Buddha's birthplace, Lumbini, Nepal: environmental implications, Environmental Science and Pollution Research, 25, 14868-14881, https://doi.org/10.1016/j.envpol.2020.114872, 2018.

Sarangi, C., Qian, Y., Rittger, K., Ruby Leung, L., Chand, D., Bormann, K. J., and Painter, T. H.: Dust dominates high-altitude snow darkening and melt over high-mountain Asia, Nature Climate Change, 10, 1045-1051, https://doi.org/10.1038/s41558-020-00909-3, 2020.

Shiraiwa, M., Ueda, K., Pozzer, A., Lammel, G., Kampf, C. J., Fushimi, A., Enami, S., Arangio, A. M., Fröhlich-Nowoisky, J., Fujitani, Y., Furuyama, A., Lakey, P. S. J., Lelieveld, J., Lucas, K., Morino, Y., Pöschl, U., Takahama, S., Takami, A., Tong, H., Weber, B., Yoshino, A., and Sato, K.: Aerosol Health Effects from Molecular to Global Scales, Environmental Science & Technology, 51, 13545-13567, https://doi.org/10.1021/acs.est.7b04417, 2017.

Skamarock, W. C., Klemp, J., Dudhia, J., Gill, D., Barker, D., Wang, W., and Powers, J.: A description of the Advanced Research WRF version 2. NCAR Tech, Note NCAR/TN-4681STR, 2005.

Takahashi, H. G., Watanabe, S., Nakata, M., and Takemura, T.: Response of the atmospheric hydrological cycle over the tropical Asian monsoon regions to anthropogenic aerosols and its seasonality, Progress in Earth and Planetary Science, 5, 44, https://doi.org/10.1186/s40645-018-0197-2, 2018.

Twomey, S.: The influence of pollution on the shortwave albedo of clouds, Journal of the atmospheric sciences, 34, 1149-1152, https://doi.org/10.1175/1520-0469(1977)034<1149:TIOPOT>2.0.CO;2, 1977.

Ukhov, A., Ahmadov, R., Grell, G., and Stenchikov, G.: Improving dust simulations in WRF-Chem model v4. 1.3 coupled with GOCART aerosol module, Geoscientific Model Development 14, 473–493, https://doi.org/10.5194/gmd-14-473-2021, 2020a.
Ukhov, A., Mostamandi, S., Krotkov, N., Flemming, J., da Silva, A., Li, C., Fioletov, V., McLinden, C., Anisimov, A., and Alshehri, Y. M.: Study of SO Pollution in the Middle East Using MERRA-2, CAMS Data Assimilation Products, and High-Resolution WRF-Chem Simulations, Journal of Geophysical Research: Atmospheres, 125, e2019JD031993, 2020b.
Uno, I., Wang, Z., Itahashi, S., Yumimoto, K., Yamamura, Y., Yoshino, A., Takami, A., Hayasaki, M., and Kim, B.-G.: Paradigm shift in aerosol chemical composition over regions downwind of China, Scientific reports, 10, 1-11, https://doi.org/10.1038/s41598-020-63592-6, 2020.
Vinoj, V. and Pandey, S. K.: Chapter 5 - Role of meteorology in atmospheric aerosols and air pollution over South Asia, in: Asian Atmospheric Pollution, edited by: Singh, R. P., Elsevier, 97-110, https://doi.org/10.1016/B978-0-12-816693-2.00018-4, 2022.
Voss, K. K., Evan, A. T., Prather, K. A., and Ralph, F. M.: Dusty Atmospheric Rivers: Characteristics and Origins, Journal of Climate, 33, 9749-9762, https://doi.org/10.1175/JCLI-D-20-0059.1, 2020.
Wang, T., Chen, Y., Gan, Z., Han, Y., Li, J., and Huang, J.: Assessment of dominating aerosol properties and their long-term trend in the Pan-Third Pole region: A study with 10-year multi-sensor measurements, Atmospheric Environment, 239, 117738, https://doi.org/10.1016/j.atmosenv.2020.117738, 2020.
Wang, X., Dickinson, R. E., Su, L., Zhou, C., and Wang, K.: PM2. 5 pollution in China and how it has been exacerbated by terrain and meteorological conditions, Bulletin of the American Meteorological Society, 99, 105-119, https://doi.org/10.1175/BAMS-D-16-0301.1, 2018a.
Wang, X., Dickinson, R. E., Su, L., Zhou, C., and Wang, K.: PM2.5 Pollution in China and How It Has Been Exacerbated by Terrain and Meteorological Conditions, Bulletin of the American Meteorological Society, 99, 105-119, https://doi.org/10.1175/BAMS-D-16-0301.1, 2018b.
Ambient (outdoor) air pollution: https://www.who.int/news-room/fact-sheets/detail/ambient-(outdoor)-air-quality-and-health, last
Wiedinmyer, C., Akagi, S., Yokelson, R. J., Emmons, L., Al-Saadi, J., Orlando, J., and Soja, A.: The Fire INventory from NCAR (FINN): A high resolution global model to estimate the emissions from open burning, Geoscientific Model Development, 4, 625, https://doi.org/10.5194/gmd-4-625-2011, 2011.
Xu, G., Ma, X., Chang, P., and Wang, L.: Image-processing-based atmospheric river tracking method version 1 (IPART-1), Geoscientific Model Development, 13, 4639-4662, https://doi.org/10.5194/gmd-13-4639-2020, 2020.
Yang, J., Kang, S., and Ji, Z.: Critical contribution of south Asian residential emissions to atmospheric black carbon over the Tibetan plateau, Science of The Total Environment, 709, 135923, https://doi.org/10.1016/j.scitotenv.2019.135923, 2020.
Yang, J., Kang, S., Ji, Z., and Chen, D.: Modeling the origin of anthropogenic black carbon and its climatic effect over the Tibetan Plateau and surrounding regions, Journal of Geophysical Research: Atmospheres, 123, 671-692, https://doi.org/10.1002/2017JD027282, 2018.
Yin, Z., Wan, Y., Zhang, Y., and Wang, H.: Why super sandstorm 2021 in North China, National Science Review, 9, https://doi.org/10.1093/nsr/nwab165, 2021.

https://doi.org/10.5194/acp-2022-199
Preprint. Discussion started: 11 April 2022

Yuan, T., Chen, S., Wang, L., Yang, Y., Bi, H., Zhang, X., and Zhang, Y.: Impacts of Two East Asian Atmospheric Circulation Modes on Black Carbon Aerosol Over the Tibetan Plateau in Winter, Journal of Geophysical Research: Atmospheres, 125, e2020JD032458, https://doi.org/10.1029/2020JD032458, 2020.

Zhang, M., Zhao, C., Cong, Z., Du, Q., Xu, M., Chen, Y., Chen, M., Li, R., Fu, Y., Zhong, L., Kang, S., Zhao, D., and Yang, Y.: Impact of topography on black carbon transport to the southern Tibetan Plateau during the pre-monsoon season and its climatic implication, Atmosheric Chemistry and Physics, 20, 5923-5943, https://doi.org/10.5194/acp-20-5923-2020, 2020a.

Zhang, Q., Zheng, Y., Tong, D., Shao, M., Wang, S., Zhang, Y., Xu, X., Wang, J., He, H., and Liu, W.: Drivers of improved PM2. 5 air quality in China from 2013 to 2017, Proceedings of the National Academy of Sciences, 116, 24463-24469, https://doi.org/10.1073/pnas.1907956116, 2019a.

Zhang, Q., Zheng, Y., Tong, D., Shao, M., Wang, S., Zhang, Y., Xu, X., Wang, J., He, H., Liu, W., Ding, Y., Lei, Y., Li, J., Wang, Z., Zhang, X., Wang, Y., Cheng, J., Liu, Y., Shi, Q., Yan, L., Geng, G., Hong, C., Li, M., Liu, F., Zheng, B., Cao, J., Ding, A., Gao, J., Fu, Q., Huo, J., Liu, B., Liu, Z., Yang, F., He, K., and Hao, J.: Drivers of improved PM_{2.5} air quality in China from 2013 to 2017, Proceedings of the National Academy of Sciences, 116, 24463, 10.1073/pnas.1907956116, 2019b.

Zhang, R., Wang, H., Qian, Y., Rasch, P. J., Easter, R. C., Ma, P.-L., Singh, B., Huang, J., and Fu, Q.: Quantifying sources, transport, deposition and radiative forcing of black carbon over the Himalayas and Tibetan Plateau, Atmospheric Chemistry & Physics Discussions, 15, 2015a.

Zhang, R., Wang, H., Qian, Y., Rasch, P. J., Easter, R. C., Ma, P. L., Singh, B., Huang, J., and Fu, Q.: Quantifying sources, transport, deposition, and radiative forcing of black carbon over the Himalayas and Tibetan Plateau, Atmosheric Chemistry and Physics, 15, 6205-6223, https://doi.org/10.5194/acp-15-6205-2015, 2015b.

Zhang, X., Chen, S., Kang, L., Yuan, T., Luo, Y., Alam, K., Li, J., He, Y., Bi, H., and Zhao, D.: Direct Radiative Forcing Induced by Light-Absorbing Aerosols in Different Climate Regions Over East Asia, Journal of Geophysical Research: Atmospheres, 125, e2019JD032228, https://doi.org/10.1029/2019JD032228, 2020b.

Zhang, Y., Ding, A., Mao, H., Nie, W., Zhou, D., Liu, L., Huang, X., and Fu, C.: Impact of synoptic weather patterns and inter-decadal climate variability on air quality in the North China Plain during 1980–2013, Atmospheric Environment, 124, 119-128, https://doi.org/10.1016/j.atmosenv.2015.05.063, 2016.

Zhao, C., Chen, S., Leung, L. R., Qian, Y., Kok, J. F., Zaveri, R. A., and Huang, J.: Uncertainty in modeling dust mass balance and radiative forcing from size parameterization, Atmosheric Chemistry and Physics, 13, 10733-10753, https://doi.org/10.5194/acp-13-10733-2013, 2013.

Zhao, C., Liu, X., Leung, L. R., Johnson, B., McFarlane, S. A., Gustafson Jr, W. I., Fast, J. D., and Easter, R.: The spatial distribution of mineral dust and its shortwave radiative forcing over North Africa: modeling sensitivities to dust emissions and aerosol size treatments, Atmosheric Chemistry and Physics, 10, 8821-8838, https://doi.org/10.5194/acp-10-8821-2010, 2010.

Zhao, S., Feng, T., Tie, X., and Wang, Z.: The warming Tibetan Plateau improves winter air quality in the Sichuan Basin, China, Atmosheric Chemistry and Physics, 20, 14873-14887, 10.5194/acp-20-14873-2020, 2020a.

https://doi.org/10.5194/acp-2022-199
Preprint. Discussion started: 11 April 2022

Zhao, S., Tie, X., Long, X., and Cao, J.: Impacts of Himalayas on black carbon over the Tibetan Plateau during summer monsoon, Science of the Total Environment, 598, 307-318, 10.1016/j.scitotenv.2017.04.101, 2017.

Zhao, S., Yin, D., Yu, Y., Kang, S., Qin, D., and Dong, L.: PM2. 5 and O3 pollution during 2015–2019 over 367 Chinese cities: Spatiotemporal variations, meteorological and topographical impacts, Environmental Pollution, 114694, 2020b.

Zhao, S., Yin, D., Yu, Y., Kang, S., Qin, D., and Dong, L.: PM(2.5) and O(3) pollution during 2015-2019 over 367 Chinese cities: Spatiotemporal variations, meteorological and topographical impacts, Environmental pollution (Barking, Essex : 1987), 264, 114694, https://doi.org/10.1016/j.envpol.2020.114694, 2020c.

Zheng, X. Y., Fu, Y. F., Yang, Y. J., and Liu, G. S.: Impact of atmospheric circulations on aerosol distributions in autumn over eastern China: observational evidence, Atmosheric Chemistry and Physics, 15, 12115-12138, https://doi.org/10.5194/acp-15-12115-2015, 2015.